1   **Mycobacterial infection of precision cut lung slices reveals that the type 1**

2   **interferon pathway is locally induced by Mycobacterium bovis but not M.**

3   **tuberculosis in different cattle breeds**

4

5   Aude Remot[1*], Florence Carreras[1], Anthony Coupé[1], Émilie Doz-Deblauwe[1],

6   Boschiroli ML[2], John A. Browne[3], Quentin Marquant[4], Delphyne Descamps[4],

7   Fabienne Archer[5], Abrahma Aseffa[6], Pierre Germon[1], Stephen V. Gordon[7], and

8   Nathalie Winter[1]

9

10   [1] INRAE, Université de Tours, ISP, 37380 Nouzilly, France.

11   [2] Paris-Est University, National Reference Laboratory for Tuberculosis, Animal Health

12   Laboratory, Anses, Maisons-Alfort, France.

13   [3] UCD School of Agriculture and Food Science, University College Dublin, Belfield,

14   Dublin 4, Ireland.

15   [4] INRAE, Université Paris-Saclay, UVSQ, VIM, 78350 Jouy-en-Josas, France.

16   [5] Université de Lyon, Université Lyon 1, INRAE, UMR754, Viral Infections and

17   Comparative Pathology, Université de Lyon, Université Lyon 1, INRAE, Lyon,

18   France.

19   [6] Armauer Hansen Research Institute, P O Box 1005, Addis Ababa, Ethiopia.

20   [7] UCD School of Veterinary Medicine and UCD Conway Institute, University College

21   Dublin, Belfield, Dublin 4, Ireland.

22

23

24   * Correspondence should be addressed to AR aude.remot@inrae.fr

25

26   **KEY WORDS:** cattle, *Mycobacterium bovis*, *ex vivo*, Precision Cut Lung Slices,

27   alveolar macrophages, type I interferon

28

29   Number of words: 6434

30   Number of figures: 7

31   Number of supplementary figures: 6

32

ABSTRACT

Tuberculosis exacts a terrible toll on human and animal health. While *Mycobacterium tuberculosis* (Mtb) is restricted to humans, *Mycobacterium bovis* (Mb) is present in a large range of mammalian hosts. In cattle, bovine TB (bTB) is a notifiable disease responsible for important economic losses in developed countries and underestimated zoonosis in the developing world. Early interactions that take place between mycobacteria and the lung tissue early after aerosol infection govern the outcome of the disease. In cattle, these early steps remain poorly characterized. The precision-cut lung slice (PCLS) model preserves the structure and cell diversity of the lung. We developed this model in cattle in order to study the early lung response to mycobacterial infection. *In situ* imaging of PCLS infected with fluorescent Mb revealed bacilli in the alveolar compartment, adjacent or inside alveolar macrophages (AMPs) and in close contact with pneumocytes. We analyzed the global transcriptional lung inflammation signature following infection of PCLS with Mb and Mtb in two French beef breeds: Blonde d'Aquitaine and Charolaise. Whereas lungs from the Blonde d'Aquitaine produced high levels of mediators of neutrophil and monocyte recruitment in response to infection, such signatures were not observed in the Charolaise in our study. In the Blonde d'Aquitaine lung, whereas the inflammatory response was highly induced by two Mb strains, AF2122 isolated from cattle in the UK and Mb3601 circulating in France, the response against two Mtb strains, H37Rv the reference laboratory strain and BTB1558 isolated from zebu in Ethiopia, was very low. Strikingly, the type I interferon pathway was only induced by Mb but not Mtb strains indicating that this pathway may be involved in mycobacterial virulence and host tropism. Hence, the PCLS model in cattle is a valuable tool to deepen our understanding of early interactions between lung host cells and mycobacteria. It revealed striking differences between cattle breeds and mycobacterial strains. This model could help deciphering biomarkers of resistance *versus* susceptibility to bTB in cattle as such information is still critically needed for bovine genetic selection programs and would greatly help the global effort to eradicate bTB.

INTRODUCTION

Bovine tuberculosis (bTB) caused by *Mycobacterium bovis* (Mb) remains one of the most challenging infections to control in cattle. Because of its zoonotic nature, this pathogen and associated notifiable disease in cattle are under strict surveillance and regulation in the European Union. When bTB cases are detected through surveillance, culling of these reactor cattle is mandatory. In spite of intensive eradication campaigns, bTB is still prevalent in European cattle [1; 2] and has significant economical, social and environmental implications. Since 2001, France is an officially bTB free country a status that was achieved through costly surveillance programs. However, each year, around one hundred Mb foci of infection are identified [3] with certain geographical areas showing a constant rise in disease prevalence since 2004.

bTB eradication is an unmet priority that faces two major difficulties: the persistence of undetected infected animals in herds because of lack of diagnostic sensitivity, and the risk of transmission from infected sources [4]. Moreover, the poor understanding of bTB pathophysiology in cattle and the lack of correlates of protection are substantial knowledge gaps that must be resolved so as to better tackle the disease (DISCONTOOLS, https://www.discontools.eu/).

Both Mb and *M. tuberculosis* (Mtb) belong to the same genetic complex. Mtb is responsible for tuberculosis (TB) in humans which displays similar features with bTB. It is estimated that one third of the global human population are latently infected with Mtb which kills 1.4 million people each year [5]. Despite the high degree of identity that Mtb and Mb share both at the genetic level as well as during the infection process, the two pathogens display distinct tropism and virulence depending on the host. While Mb is highly virulent and pathogenic for cattle and a range of other mammals, Mtb is restricted to sustain in humans. Experimental infection of cattle with the widely used Mtb laboratory strain H37Rv, which was genome sequenced in 1998 [6], shows strong attenuation as compared to Mb [7; 8]. However, natural infection of cattle with Mtb has been reported, and the strain Mtb BTB1558 was once such case, isolated from a zebu bull in Ethiopia [9; 10]. In comparison to the original UK Mb strain AF2122/97, the first genome sequenced Mb isolate [11; 12], the Mtb strain BTB1558 diplayed much lower virulence in European cattle [13].

98

99 The Mb strains that circulate in France today are phylogenetically distant from the UK
100 Mb reference strain. While AF2122 belongs to the European 1 clonal complex [14],
101 the European 3 clonal complex is widespread in France, [15]. The Eu3 genetic
102 cluster is composed of field strains that share the SB0120 spoligotype with the
103 attenuated Bacillus Calmette Guérin vaccine strain [16; 17]. In our study, we used
104 Mb3601 as the representative strain of this widespread French cluster. Originally,
105 Mb3601 was isolated from a tracheobronchial lymph node of an infected bovine in a
106 bTB highly enzoonotic area in France [16]. However, despite widespread circulation
107 in its origine area, nothing is known today of the pathophysiology of Mb3601
108 infection.

109 Indeed, greater knowledge is available on Mtb infection process and disease
110 development both in humans and mouse models as compared to Mb infection in
111 cattle. With both mycobacteria, the alveolar macrophage (AMP) is the frontline cell
112 that first presents the first niche for mycobacteria entering the lung, and the role of
113 the AMP in early-stage infection is well established [8]. Both Mtb and Mb have
114 established their lifestyle in AMPs: they can escape its bactericidal mechanisms and
115 multiply within this niche. During the infection process, bacilli disseminate to different
116 anatomical sites and establish new infection foci both in the lungs and secondary
117 lymphoid organs [18; 19]. During Mtb infection, lung epithelial cells also play key
118 roles in the host defense (reviewed in [20; 21; 22]). Type II pneumocytes are infected
119 by Mtb [23] and produce pro-inflammatory cytokines which augment the AMP innate
120 resistance mechanisms [24]. The role of Type II pneumocytes during Mb infection in
121 cattle is not well known. Also, most of the available knowledge on the role of bovine
122 macrophages (MPs) during Mb infection comes from studies conducted with
123 monocytes sampled from blood and derived as MPs during *in vitro* culture [25].

124

125 In our study, we wanted to investigate the bovine innate response following Mb or
126 Mtb infection in a preserved lung environment to allow the resident lung cells to
127 interact with bacilli and crosstalk. Precision cut lung slices (PCLS) are an
128 experimental model in which resident lung cell types are preserved and remain alive
129 for at least one week [26]. The tissue architecture and the interactions between the
130 different cells are maintained. PCLS have already been validated for the study of
131 various respiratory pathogens [26; 27; 28]. In chicken PCLS, mononuclear cells are

4

132   highly motile and actively phagocytic [29]. This model is well designed to study

133   complex interactions taking place early after the host-pathogen encounter. During Mb

134   infection in cattle, important differences in production of key proinflammatory

135   cytokines such as IFNγ or TNFα by peripheral blood mononuclear cells are observed

136   depending on the clinical status of the animal. Interestingly, such differences are

137   observed at early time points [30] indicating that the innate phase of the host reponse

138   is key to the establishment of the pathological outcome of the infection.

139

140   Therefore the PCLS model is ideally suited to investigate early host-pathogen

141   interactions in the bovine lung during Mb infection, and may help to find clues to the

142   impact of the innate response on the outcome of infection. This model, that fully

143   mimicks the early environment of the bacillus entering the lung (as compared to

144   monocyte-derived MPs) may also aid in understanding the molecular basis of

145   mycobacterial host preference [31]. To this end, we decided to compare four

146   mycobacterial strains: two Mtb species, namely the Mtb H37Rv reference strain for

147   human TB and the cattle-derived Mtb BTB1558, and two Mb species namely Mb

148   AF2122 as representative of the EU1 clonal complex and Mb3601 as the hallmark

149   EU3 strain. Since the host genetic background also has profound impact on the

150   outcome of bTB disease [32], we decided to compare PCLS from two prevalent beef

151   breeds in France, Charolaise and Blonde d'Aquitaine, and conducted a thorough

152   characterization of the lung responses to Mb and Mtb during *ex vivo* infection. PCLS

153   allowed us to decipher important differences in the transcriptomic and cytokine profile

154   during the innate response to infection, depending both on the breed, i.e. between

155   Blonde d'Aquitaine and Charolaise cows, and on the mycobacterial species, i.e.

156   between Mtb and Mb.

157

158   **MATERIALS AND METHODS**

159   **Animal tissue sampling**

160   Lungs from fifteen Blonde d'Aquitaine and nine Charolaise cows were collected post-

161   mortem at a commercial abattoir. Animals were between three- and eleven-years-old

162   and originated from eight different French departments where no recent bTB

163   outbreak had been notified (Figure S1). No ethical committee approval was

164   necessary as no animal underwent any experimental procedure. After slaughter by

165   professionals following the regulatory guidelines from the abattoir, the lungs from

166   each cow were systematically inspected by veterinary services at the abattoir. The
167   origin of each animal was controlled and its sanitary status was recorded on its
168   individual passport: animals were certified free of bTB, leucosis, brucellosis, and
169   infectious bovine rhinotracheitis.
170
171   **Bacterial strains and growth conditions**
172   Strains Mb AF2122/97 and Mb MB3601 had previosuly been isolated from infected
173   cows in Great Britain and France, respectively [12; 15]. The Mb3601-EGFP
174   fluorescent strain were derived by electroporation with an integrative plasmid
175   expressing EGFP and selected with Hygromycin B (50 μg/mL) (Sigma, USA) as
176   described in previously [33]. Mtb BTB1558 had been previosuly isolated from a zebu
177   bull in Ethiopia [13]. Bacteria were grown in Middlebrook 7H9 broth (Difco, UK)
178   supplemented with 10% BBLTM Middlebrook ADC (Albumin- Dextrose- Catalase,
179   BD, USA) and 0.05% Tween 80 (Sigma-Aldrich, St Louis, USA). At mid-log phase,
180   bacteria were harvested, aliquoted, and stored at -80°C. Batches titers were
181   determined by plating serial dilutions on Middlebrook 7H11 agar supplemented with
182   10% OADC (Oleic acid- Albumin-Dextrose-Catalase, BD, USA), with 0.5% glycerol or
183   4.16 g/L sodium pyruvate (Sigma, USA) added for Mtb or Mb strains, respectively.
184   Plates were incubated at 37°C for 3-4 weeks (H37Rv, BTB558 and AF2122) and up
185   to 6 weeks for Mb3601 before CFUs numeration. Inocula were prepared from one
186   frozen aliquot (titer determined by CFU numeration) that was thawed in 7H9 medium
187   without glycerol and incubated overnight at 37°C. After centrifugation 10 min at 3000
188   x g, concentration was adjusted to 10^6 cfu/mL in RPMI medium.
189
190   **Obtention and infection of Precision-Cut Lung Slices (PCLS)**
191   PCLS were obtained from fresh lungs using a tissue slicer MD 6000 (Alabama
192   Research and Development). For each animal, the right accessory lobe was filled via
193   the bronchus with RPMI containing 1.5% low melting point (LMP) agarose
194   (Invitrogen) warmed at 39°C. After 20 min at 4°C, solidified lung tissue was cut in 1.5
195   cm slices with a scalpel. A 0.8 mm diameter punch was used to obtain biopsies that
196   were placed in the microtome device of the Krumdieck apparatus, filled with cold
197   PBS, and 100 μM thick PCLS were cut. One PCLS was introduced in each well of a
198   P24 well plate (Nunc), one mL of RPMI 1640 (Gibco) supplemented with 10% heat
199   inactivated Fetal Calf Serum (FCS, Gibco), 2 mM L-Glutamine (Gibco) and PANTA™

6

200 Antibiotic Mixture (polymyxin B, amphotericin B, nalidixic acid, trimethoprim and
201 azlocillin; Becton Dickinson) was added to the well and the plate was incubated at
202 37°C with 5% CO_2. Medium was changed every 30 min during the first 2 h to remove
203 all traces of LMP agarose. Twenty four hours later, after the last medium change, the
204 ciliary activity was observed under a microscope to ensure tissue viability.

205

206 PCLS were infected two days with 10^5 CFU of Mb or Mtb strains. As indicated, PCLS
207 were either fixed in formalin for imaging or lyzed with a Precellys in lysing matrix D
208 tubes in 800 µL Tri-reagent for RNA extraction. The bacillary load of each strain
209 present in the PCLS was compared after transfer of PCLS to a new plate 1 day after
210 infection (dpi), two washes in 1 mL of PBS, and homogenization in 1 mL of PBS in
211 lysing matrix D tubes (MP Biomedicals) with a Precellys (Ozyme). To determine
212 CFUs, serial dilutions were plated as described above.

213

214 **Alveolar macrophages (AMPs)**
215 To harvest AMPs from Blonde d'Aquitaine cows, broncho-alveolar lavages (BAL)
216 were performed on the left basilar lobe of the lung at a local abattoir after culling of
217 the animal. The lobe was filled with 2 x 500mL of cold PBS containing 2 mM EDTA
218 (Sigma-Aldrich). After massage, the BAL was collected and transported at 4°C to the
219 laboratory. BAL was filtered with a 100 µm cell strainer (Falcon) and centrifuged for
220 10 min at 300 x g. Cells were washed in RPMI medium supplemented with 10% heat
221 inactivated fetal calf serum (Gibco), 2 mM L-Glutamine (Gibco) and PANTA™
222 Antibiotic Mixture. 10^7 BAL cells per mL were suspended in 90% FCS and 10%
223 DMSO (Sigma-Aldrich) and cryopreserved in liquid nitrogen. One day before
224 infection, BAL cells were thawed at 37°C, washed in complete RPMI medium, and
225 transferred to a 75 cm² culture flask with a ventilated cap. After 2 h at 37°C 5% CO_2,
226 non adherent cells were removed, and adherent AMPs were incubated 2 x 10min at
227 4°C with 10 mL of cold PBS to detach and enumerate them in a Malassez chamber.
228 5 x 10^5 AMPs /well were distributed in a P24 well-plate and incubated overnight at
229 37°C 5% CO_2. Medium was changed once and AMPs were infected with Mb3601 or
230 Mtb H37Rv at a MOI of 1. At 6 h and 24 h pi, supernatants were filtered through a 0.2
231 µm filter and cells were lyzed in 800 µL of Tri-reagent for RNA extraction. MOI was
232 checked by CFU determination 24 h after infection.

233

Cell supernatant collection and lactate deshydrogenase (LDH) assay

In order to evaluate cytotoxicity, supernatants from infected PCLS or AMPs were passed through a 0.2 µm filter at indicated time points and cells were lysed in 1 mL of lysis buffer (5mM EDTA, 150 mM NaCl, 50 mM Tris-HCl, Triton 1%, pH 7,4), containing anti-proteases (Roche), in lysing matrix D tube, with a Precellys apparatus. Homogenates were clarified by centrifugation 10 min at 10000 x g, filtered through 0.2 µm and collected on microplates. Cytotoxicity of infection in PCLS was assessed using the "Non-Radioactive Cytotoxicity Assay" kit (Promega) according to the manufacturer's instructions. The cytotoxicity was calculated as: cytotoxicity (%) = (OD_{490} of LDH in the supernatant)/(OD_{490} of LDH in the supernatant + OD_{490} of LDH in the PCLS homogenates) x 100.

Immunohistochemistry on PCLS

Infected PCLS were fixed 24 h at 4°C with 4% of formalin, then transfered to a 48-wells culture plate in PBS. All steps described below were done under gentle agitation at room temperature (RT). PCLS were incubated 2 h with 100 µL of PBS, 0.25% Triton X-100, 10% horse serum for permeabilization and saturation (saturation buffer). They were incubated overnight at 4°C with primary Ab (anti-bovine MHCII clone MCA5655 from BioRad, anti-bovine pancytokeratine clone BM4068 from Acris) diluted in saturation buffer. PCLS were washed 4 times with 300 µL of PBS (2x 5 min, then 2x 10 min), then incubacted 3 h with fluorescent-conjugated secondary antibodies diluted in saturation buffer (Goat anti-mouse IgG1-APC and Goat anti-mouse IgG2a A555 from Invitrogen). PCLS were washed 4 times with 300 µL of PBS (2x 5 min, then 2 x 10 min), and transfered on coverslides which were mounted with Fluoromount-G™ Mounting Medium, containing DAPI (Invitrogen) and sealed with transparent nail polish. Z-stack imaging was performed at x 63 enlargment with a confocal microscope (LEICA) and analyzed with LAS software.

Quantification of cytokines and chemokines released by PCLS and AMPs

Cytokine and chemokine levels produced by PCLS after 2 dpi were assessed in a Multiplex assay in supernatants (dilution 1:2) with MILLIPLEX® Bovine Cytokine/Chemokine Panel 1 (BCYT1-33K-PX15, Merck) according to the manufacturer's instructions. IFNγ, IL-1α, IL-1β, IL-4, IL-6, IL-8 (CXCL8), IL-10, IL-17A, IL-36RA (IL-1F5), IP-10 (CXCL10), MCP-1 (CCL2), MIP-1α (CCL3), MIP-1β

8

268   (CCL4), TNFα, & VEGF-A were measured. Data were acquired using a MagPix

269   instrument (Luminex) and analyzed with Bio-Plex Manager software (Bio-Rad). IL-8

270   was out of range in the Multiplex, so we performed a sandwich ELISA with the

271   following references: Goat anti Bovine Interleukin-8 Ab AHP2817, Recombinant

272   Bovine Interleukin-8 PBP039 and Goat anti Bovine Interleukin-8 Ab conjugated to

273   biotin AHP2817B (all from Bio-Rad, protocol according to the manufacturer's

274   intructions).

275

276   **RNA extraction and gene expression analysis**

277   Total RNA from two pooled PCLS were extracted using a MagMAX™-96 Total RNA

278   isolation kit (ThermoFisher). For AMPs we used the Nucleospin RNA isolation kit

279   (Macherey Nagel). After DNase treatment (ThermoFisher or Macherey Nagel)

280   mRNAs were reverse transcribed with iScript™ Reverse Transcriptase mix (Biorad)

281   according to the manufacturer's instructions. Primers (Eurogenetec; Supplementary

282   Table S1) were validated using a serially diluted pool of cDNA mix obtained from

283   bovine lung, lymph nodes, blood and bone marrow, with a LightCycler® 480 Real-

284   Time PCR System (Roche). Gene expression was then assessed with the

285   BioMark HD (Fluidigm) in 96 x 96 well IFC plate, according to the manufacturer's

286   instructions. The annealing temperature was 60°C. Data were analyzed with Fluidigm

287   RealTime PCR software to determine the cycle threshold (Ct) values. Messenger

288   RNA (mRNA) expression was normalized to the mean expression of three

289   housekeeping genes (*PPIA, GAPDH, ACTB*) to obtain the ΔCt value. For each

290   animal, values from infected PCLS were normalized to the uninfected PCLS gene

291   expression (ΔΔCt value, and Relative Quantity = $2^{-\Delta\Delta Ct}$). Principal Component

292   Analysis (PCA) were performed using ΔΔCt values in R studio (Version 1.1.456 ©

293   2009-2018 RStudio, PBC), using the FactoMineR packages (version R 3.5.3).

294

295   **Statistical analysis**

296   Individual data, and the median and interquartile range are presented in the figures,

297   exept for Figure 2 where the mean and standard deviation are presented. Statistical

298   analyses were performed with Prism 6.0 software (GraphPad). Analyzes were

299   performed on data from two to six independent experiments, with 2-way ANOVA or

300   Wilcoxon non-parametric tests for paired samples used. Represented p-values were:

301   $*p < 0.05; **p < 0.01; ***p < 0.001$.

302

SUPPLEMENTARY INFORMATION

The Supplementary Material for this article can be found online.

305

RESULTS

307

***Ex vivo* infection with mycobacteria of live bovine lung tissue in PCLS allows bacilli uptake by AMPs and their recruitment to alveoli.**

Early events of bTB pathophysiology in the bovine lung remain poorly defined due to the complexity of biocontained experimental infection in large animals. Since PCLS have been used to study viral respiratory infections in the bovine [26], we decided to use this model to assess early events taking place following entry of Mb into the lung. We infected bovine PCLS obtained *ex vivo* with the four mycobacterial strains: Mb AF2122, Mb3601, Mtb H37Rv or BTB1558.

316

We first monitored tissue cytotoxicity at 1 and 2 days post infection (dpi) using a lactate deshydrogenase (LDH) release assay. The mean percentage of cytotoxicity remained below 10% and no difference was observed between infected and non-infected PCLS (Fig. 1A). The ciliary activity from the PCLS bronchial cells monitored every day under a light microscope remained vigourous and stable after infection (data not shown). We calibrated our model and inocula to use 10^5 CFUs for each of the four different strains. We analyzed CFUs still present in PCLS 24 h later and observed an equivalent 1 log decrease for all strains (Fig. 1B). This indicated equivalent infection by all strains, allowing them to be directly compared. Therefore, with similar bacterial load and excellent tissue viability in all experimental conditions, we validated PCLS as a model to study early events taking place in the bovine lung after infection with mycobacteria.

329

In order to visualize interactions taking place between bacilli and lung cells, we infected PCLS with a fluorescent version of the Mb3601 strain, and at 1 and 2 dpi we analyzed the cells by *in situ* immunohistochemistry. The lung structure was visualized by DAPI and pancytokeratine staining and we used confocal microscopy to image 10-15µm sections and localize Mb3601-EGFP (Fig. 2A). We observed Mb in 27 ± 3 % of PCLS alveoli (Fig. 2A and 2B) and almost always in close contact with large

10

336 MHC-II positive AMPs. Bacilli were localized outside AMPs in 76 ± 2 % observations
337 and resided intracellularly in AMPs in 24 ± 2 % (Fig. 2A and 2C and Supplementary
338 video). Interestingly, the number of AMPs per alveoli differed upon bacilli presence or
339 absence (Fig. 2D). In uninfected PCLS, lung alveoli generally contained one AMP
340 (data not shown). However, in Mb infected PCLS, we either observed no AMPs in 66
341 ± 2 % of alveoli or one AMP in 33 ± 2 % of alveoli in the absence of any Mb. On the
342 contrary, the number of AMPs significantly increased in alveoli where at least one Mb
343 was observed (Fig. 2D, $p<0.001$). The number of AMPs varied among infected
344 alveoli with 24 ± 9 % containing one AMP, 52 ± 6% containing 2 or 3 AMPs and 9 ± 4
345 % containing more than 4 AMPs. Such observations indicated that during the 2 days
346 of infection, AMPs were recruited from one alveoli to the other in response to signals
347 linked to Mb infection. In conclusion, even though Mb infection was performed *ex*
348 *vivo*, bacilli were observed in the alveoli, close or inside their target host cell i.e. the
349 AMP. Moreover, the PCLS model was physiological enough to allow AMPs to crawl
350 in response to signals linked to bacilli entry.

351

352 **The lung response to mycobacterial infection vastly differs between Blonde**
353 **d'Aquitaine and Charolaise cows.**
354 Two bovine beef breeds are widely used in France: Blonde d'Aquitaine and
355 Charolaise. We decided to compare how these two breeds respond to mycobacterial
356 infection, using our PCLS system. We measured 15 cytokines and chemokines
357 secreted by the lung tissue at 2 dpi with the four mycobacterial strains and performed
358 a principal component analysis (PCA). As depicted in Fig. 3A, PCA revealed
359 important differences in the immune response of the lung tissue between the two
360 breeds. Group samples clearly plotted appart and their ellipses showed either a small
361 overlay (AF2122 and Mb360A) or no overlay at all (H37Rv). Results for the BTB1558
362 group showed less clustering of samples due to higher individual variations. We then
363 extracted total RNA from PCLS after 1 or 2 dpi and analyzed the expression of 96
364 genes related to innate immunity and inflammation (see full list in supplementary
365 Table 1). RT-qPCR data were normalized and expressed as fold change compared
366 to uninfected PCLS control for each cow. Gene expression was higher 2 days after
367 infection as compared to 1 (data not shown). We therefore decided to focus our
368 analysis on this 2 dpi time point. Remarkably, the transcriptomic signature induced by
369 infection was very low for the Charolaise breed, whichever mycobacterial strain was

11

370   used, which explains the clustering of Charolaise samples (Fig. 3B). Increasing the

371   inocumlum in the Charolaise PCLS up to 5×10^6 CFU did not induce gene

372   expression (Fig. S2). The response of the lung tissue to mycobacterial infection in

373   Blonde d'Aquitaine was very different as compared to Charolaise, as revealed by a

374   PCA (Fig. 3B). Whereas in PCLS from Charolaise gene expression from infected and

375   non-infected controls clustered, in PCLS from Blonde d'Aquitaine, gene expression

376   levels were significantly more dispersed after infection as compared to controls (Fig

377   3B). We compared individual gene expression between the two breeds for a number

378   of genes. For instance, both the *CXCL2* chemokine, and the mycobacteria receptor

379   syndexin 4 *SDC4*, were significantly upregulated after PCLS infection with AF2122,

380   Mb3601 or H37Rv in Blonde d'Aquitaine, but not in Charolaise (Fig. 3C). Altogether,

381   our data revealed important differences in the early lung response to mycobacterial

382   infection, depending on the breed of the animals, that could be measured both at the

383   gene expression and protein production level in the PCLS system.

384

385   **The overall inflammation signature in the lung tissue is triggered more**

386   **efficiently by *M. bovis* than *M. tuberculosis***

387   We then focused our analysis on Blonde d'Aquitaine to determine how the lung

388   tissue responded to different mycobacterial strains. We analyzed 15 cytokines and

389   chemokines produced in the PCLS supernatants 2 days following infection. No IL-4

390   was detected and production of TNFα, IL-36RA, IL-10, VEGFA or MCP-1 was not

391   different between infected PCLS and controls (Figure S3A). We observed that *ex*

392   *vivo* infection of PCLS with mycobacteria triggered an inflammatory response that

393   contrasted between the strains (Fig. 4A). At the protein level, the Mtb strain BTB1558

394   induced the most heterogenous response and, due to high individual variation,

395   differences in chemokine/cytokine production between infected PCLS and controls

396   only reached statistical signficance for MIP-1a (CCL3) and IL-8 (Fig. 4A). These two

397   inflammatory mediators were also strongly induced by all strains. IL-17A, IL-1β and

398   IFNγ were efficiently induced by mycobacterial infection and no significant difference

399   was observed between Mtb and Mb. By contrast, IL-6 and IL-1α were significantly

400   induced after Mb but not Mtb infection and IL-8 production was also significantly

401   higher after Mb than Mtb infection (Fig 4A). The only strain able to induce significant

402   production of MIP-1b was Mb3601. We then analyzed the inflammatory

403   transcriptomic signature using a panel of 17 genes involved in

404   monocyte/macrophage and neutrophil recruitment (Fig. 4B). A number of these
405   genes was significantly upregulated upon PCLS infection even though significant
406   differences were not always reached due to inter-individual variation. Remarkably,
407   Mb3601 induced the strongest inflammatory response, with 5 out of 17 genes
408   significantly upregulated as compared to non-infected controls. Focusing on
409   chemokines involved in neutrophil recruitment, we observed that *CXCL2* expression
410   was induced by all strains -except BTB1558- whereas *CXCL1*, *CXCL5* and *CXCL8*
411   were only upregulated by Mb3601 (Fig. 4B and 4C). *IL-6* expression was also high
412   after Mb3601 infection. Therefore, *ex vivo* infection of PCLS efficiently triggered
413   signals involved in monocyte and neutrophil recruitment. Infection by Mb strains, and
414   more specifically the Mb3601 strain circulating in France, triggered inflammation in
415   the bovine lung more efficiently than Mtb.

416

417   **The type I interferon pathway is induced in the bovine lung by infection with *M.***
418   ***bovis* but not *M. tuberculosis***
419   Because in humans and mouse models, susceptibility to mycobacterial infection and
420   disease progression is driven by type I IFN [34; 35; 36], we decided to compare
421   induction of this pathway by Mtb and Mb strains in bovine lung tissue. We measured
422   expression of different genes involved in the type I IFN pathway in Blonde
423   d'Aquitaine PCLS infected by the four mycobacterial strains (Fig. 5). Gene
424   expression of both *IFNβ* and the *IFNAR1* receptor were significantly increased after
425   Mb but not Mtb infection (Fig. 5A and 5C). Similarly, the major IFN stimulated genes
426   (ISG) *MX1*, *OAS1*, *ISG15* and *CXCL10*, were induced only after Mb infection (Fig. 5A
427   and 5C) and this difference was also detected at the protein level for CXCL10 (Fig.
428   5A and 5B). Therefore we observed induction of a number of genes of the type I IFN
429   pathway, recapitulated in Fig 5D, after infection with Mb but not Mtb strains.
430   Strikingly, strain Mb3601 was the highest inducer of this pathway in the lung from
431   Blonde d'Aquitaine cows.

432

433   Because AMPs are the most promiment host cell interacting with Mb [8], which we
434   also observed in PCLS (Fig. 2), we next decided to decipher if AMPs contributed to
435   induction of the type I IFN pathway after Mb3601 or H37Rv infection. One day after
436   infection of AMPs with these two strains similar bacterial levels were recovered (data
437   not shown). At 6 hours post infection no cell cytotoxicity was observed and we

438 analyzed expression of genes from the type 1 IFN pathway at this early time point.
439 While we did not observe differences in *IFNAR1*, *IRF3*, *STAT1* nor *ISG15* expression
440 induced by the two strains (Fig. 6A), *IFNβ, LPG2, RIG1* and *OAS1* were significantly
441 induced after infection with Mb3601 but not H37Rv (Fig. 6C and 6D). Regarding
442 *MX1*, the same trend was observed although statistical significance was not reached
443 (Fig. 6D, *p*=0.07).

444

445 Interestingly, while CXCL10 was detected both at the mRNA and protein level in
446 PCLS infected with Mb (Fig. 5), we did not detect expression of this gene by AMPs in
447 our analysis. Altogether these results demonstrate that AMPs globally contribute to
448 the type I IFN pathway in the lung after Mb infection, although other cells present in
449 PCLS may also specifically induce some genes, such as *CXCL10* or *IRF7* for
450 example (Fig. 5C and 6A).

451

452 **DISCUSSION**
453 The lung is the main organ targeted by Mb infection in cattle [37] and early
454 interactions between the different lung cell types and the bacillus that govern the
455 pathophysiology of the disease need to be better understood. In this study we used
456 PCLS for the first time to monitor the early bovine lung response to Mb infection, and
457 validated this model as a means to measure the local innate respoense at the protein
458 and mRNA level. A main advantage of PCLS is conservation of the complex lung
459 tissue both in structure and diversity of cell types. After infection with mycobacteria,
460 ciliary activity of bronchial cells was maintained. AMP main function is to patroll the
461 lung, crawling in and between alveoli, they sensed, chemotaxed, and phagocytosed
462 debris or inhaled bacterial [38]. We observed increased numbers of AMPs in alveoli
463 where Mb was present, indicating AMP mobility inside the tissue. In chicken, PCLS
464 allowed observation of MPs movement and phagocytosis [29]. The AMP is well
465 established as the main host cell for Mtb infection in humans [39] and Mb infection in
466 cattle [40]. Accordingly, in PCLS we observed Mb inside AMPs in 20% of infected
467 alveoli. We sometimes observed several bacilli inside one AMP. Although Mb is able
468 to replicate inside this hostile cell, it is difficult to know if this observation was due to
469 bacillary multiplication or phagocytosis of several bacilli. This issue would need live
470 imaging of PCLS to follow the fate of fluorescent Mb, an approach which remains
471 challenging under BSL3 conditions.

14

472

473 In uninfected PCLS, we observed generally one AMP for 2-3 alveoli (Fig S4, in good

474 correlation with Neupane et al., [38]). After Mb infection, we observed several AMPs

475 inside the same alveolus in 50% cases. Moreover, when the alveoli contained more

476 than four AMPs, they were in closed contact. Multinucleated giant cells are formed by

477 fusion of several MPs and are a hallmark of TB pathophysiology. It has recently been

478 demonstrated that after infection of human or bovine blood derived MPs by Mb or

479 Mtb, only Mb was able to induce the formation of multinucleated cells [41]. Although

480 2 dpi we did not observe formation of such cells in PCLS, it would be interesting to

481 analyze if such events could be detected after longer infection periods.

482

483 One other advantage of our model is the preserved diversity of lung cell composition.

484 PCLS contain type I and type II pneumocytes, endothelial cells, and bronchial cells

485 (Fig S4) and also produce key molecules like surfactant which has an established

486 role in Mtb uptake [42]. Mtb is also capable of invading type II alveolar epithelial cells

487 [23] that play important roles in host defense [20; 21; 22]. In our study, we did not

488 observe intraepithelial Mb, but specific labelling of bovine epithelial cells would be

489 required to investigate interactions between bovine lung pneumocytes and Mb in

490 more detail. However, as we observed that infected AMPs were in close contact with

491 epithelial cells in PCLS, this model will allow a more refined analysis of the crosstalk

492 between AMPs and pneumocytes during Mb infection [24].

493

494 One limitation of the PCLS model is the lack of recruitment of immune cells from

495 circulating blood. During mycobacterial infection, in response to local signals, a

496 variety of immune cells are recruited to the infection site to form the mature

497 granuloma that constrains bacillary multiplication. How this reponse is orchestrated at

498 the level of the lung tissue in cattle remains poorly established. Neutrophils, together

499 with other innate cells such as macrophages, γδ-T lymphocytes and natural killer

500 cells, were recently identified as key immune cells in early containment of infection

501 [43] and development of early lesions [44]. Moreover, humans regularly exposed to

502 Mtb, or cattle exposed to Mb, do not always develop signs of infection, i.e. remain

503 negative in IFNg-release assay or skin testing. In humans, such resistance to

504 infection through successful elimation of bacilli could be mediated by neutrophils [45].

505 Similarly, in cattle experimentally infected with Mb, some contact animals resist

15

506 infection while others develop lesions due to productive infection [46]. It is possible

507 that neutrophils could also play an important role in early elimination of Mb in cattle

508 [43]. Immune signals involved in early recruitment of neutrophils to the lung after

509 entry of Mb need to be better understood in cattle. It is known that epithelial cells

510 secrete, among other cytokines and chemokines, MIP1 and CXCL8 that attract MPs

511 and neutrophils to the site of infection. Interetingly we measured important

512 differences in production of such mediators by PCLS in response to different strains

513 of mycobacteria that could be linked to variable virulence. Although one cattle Type II

514 pneumocyte cell line has been described [47], such transformed cells are less

515 physiologically relevant than primary cells. Thus, PCLS could help understanding the

516 early orchestration of the local inflammatory response in the lung in response to

517 mycobacterial infection.

518

519 Resistance to bTB is linked to the host genetics. Zebu breeds (*Bos indicus*) have

520 been reported to be more resistant than Bos taurus derived breeds to bTB disease

521 [48]. Our results with PCLS, as a physiological model of the early lung response to

522 infection, demonstrated striking differences between Blonde d'Aquitaine and

523 Charolaise emphasizing the importance of the host genetics in response to Mb. It is

524 not known whether the stronger inflammatory response of the Blonde d'Aquitaine

525 tissue is associated with greater sensitivity or resistance to Mb infection. While robust

526 immunological responses are associated with increased pathology at the level of the

527 animal [30], at the cellular level, blood derived MPs from animals with greater

528 resistance to bTB (and that kill BCG more efficiently than cells from susceptible

529 animals) produce higher levels of the pro-inflammatory mediators iNOS, IL-1β,

530 TNFα, MIP1 and MIP3 [49]. Although genetic selection of cattle would greatly

531 complement bTB management and surveillance programs to control and ultimately

532 eradicate the disease, especially in countries with the highest burden [50; 51],

533 biomarkers to evaluate resistance or susceptibility of cattle to Mb infection are

534 critically missing. Some genomic regions and candidate genes have been identified

535 in Holstein Friesian cows, the most common dairy breed [52] and not surprisingly,

536 these candidates are often involved in inflammation. A genomic region on

537 chromosome 23, containing genes involved in the TNFα/NFκ-B signalling pathway,

538 was strongly associated with host susceptibility to bTB infection [53]. However, large

539 within-breed analyses of Charolaise, Limousine, and Holstein-Friesian cattle

540   identified 38 SNPs and 64 QTL regions associated with bTB susceptibility to infection

541   [54]. The genotyping of 1966 Holstein-Friesian dairy cows that were positive by skin

542   test and either did, or did not, habour visible bTB lesions, together with their skin-test

543   negative matched controls led to the conclusion that these variable phenotypes

544   following Mb exposure were governed by distinct and overlapping genetic variants

545   [55]. Thus, variation in the pathology of Mb seems to be controlled by a large number

546   of loci and a combination of small effects. Similar conclusions were drawn from

547   genetic studies of human tuberculosis [56]. In areas where Mb is highly prevalent,

548   recurrent exposure to Mb may also imprint the bovine genome, and epigenetics could

549   also contribute to the immune response in certain breeds. In France, the Nouvelle

550   Aquitaine region accounted for 80% of Mb outbreaks last year. Interestingly, Blonde

551   d'Aquitaine breed is very abundant in this area (Fig. 7). Together with another very

552   abundant beef breed in this region, Limousine, they contribute to most bTB outbreaks

553   in   Nouvelle   Aquitaire   (bovine   tuberculosis   national   reference   laboratory

554   communication). Future comparisons with Limousine would be interesting. In our

555   study, Blonde d'Aquitaine or Charolaise cows were sampled from eight different

556   French departments, none with recurrent Mb outbreaks, rendering previous exposure

557   to Mb unlikely. Moreover breeding management was similar for the two breeds, as far

558   as we could ascertain, suggesting that exposure to environment and possible wildlife

559   sources would be comparable. We nevertheless observed striking differences in the

560   early lung response to Mb infection between these two breeds, pointing to possible

561   control of Mb infection at the genetic or epigenetic level. Whether one cattle breed is

562   more susceptible to bTB than others remains an open question that deserves future

563   studies, with more consequent animal sampling to better sustain our observations.

564   We furthermore believe that the PCLS model could greatly contribute to unravelling

565   the role of tissue-level protective responses that would in turn reveal important

566   biomarkers.

567

568   In addition to the cattle breed, our study pointed towards differences in the host

569   response to distinct mycobacterial strains. Mb strains were better inducers of a lung

570   immune response than Mtb in cattle, in agreement with previous work showing that

571   Mtb H37Rv was attenuated *in vivo* in cattle as compared to Mb AF2122 [13]. *In vitro*

572   studies with bovine AMPs infected with AF2122 or H37Rv revealed differences in the

573   innate cytokine profiles: CCL4, IL-1β, IL-6 and TNFα levels were more elevated in

574 response to AF2122 than H37Rv [8], in agreement with our data. Interestingly,
575 Mb3601, a representative strain of a highly successful genetic cluster that circulates
576 both in cattle and wildlife in France [16] induced an inflammatory signature in the lung
577 more efficiently than Mb AF2122. Whether this correlates with differences in Mb
578 virulence in cattle or other mammals remains to be shown; but if this were the case,
579 the PCLS model would be a practical tool to study and compare the virulence of Mb
580 field strains, as compared to *in vivo* experimental infection of cattle. Contrary to Mtb
581 which is mostly restricted to humans, Mb is adapted to sustain across a large host
582 range through repeated cycles of infection and transmission [57; 58]. This
583 remarkable trait is due to pathogen molecular genetic changes [59] that allow
584 adapted bacilli to manipulate the host immune response to establish infection and
585 disease, and ultimately transmit infection to new, susceptible hosts [60; 61]. We
586 observed weaker inflammation in the bovine lung after infection with Mtb as
587 compared to Mb and it will be interesting to compare the ability of Mtb and Mb to
588 induce inflammation in human PCLS obtained post surgery. This latter comparative
589 analysis could give clues on the links between lung innate inflammatory responses
590 and host-adaptation during TB.
591
592 Our most striking observation was the Mb-restricted induction of the type I IFN
593 pathway in the bovine lung. This is in agreement with previous studies in bovine
594 AMPs where cytosolic DNA-sensing pathways, in particular RIG-I, were activated
595 after 48h of infection by Mb AF2122 but not Mtb H37Rv [31]. In agreement with our
596 data these authors also demonstrated induction of the RIG-I signaling pathway by Mb
597 in AMPs [62]. Therefore, AMPs contribute to type I IFN signalling in the lung.
598 However, we also noticed differences between PCLS and AMPs in induction of the
599 IFN signature by Mb: for example, CXCL10 was detected in PCLS but not in AMPs in
600 our study, which may be due to the time point used [63]. However, it is also possible
601 that other cells involved in crosstalk with AMPs contributed to CXCL10 production in
602 response to Mb infection. Since CXCL10 has been proposed as a diagnostic
603 biomarker of Mb infection in cattle [64], it will be interesting to better understand how
604 this key mediator is regulated. Type I interferon favors Mb survival and its induction
605 may be a good manipulation strategy for maintenance of infection. This manipulation
606 mechanism, deciphered *in vitro* in murine bone marrow monocyte-derived MPs,
607 involves triggering of autophagy by cytosolic Mb DNA in turn inducing IFNβ

608 production. Autophagy antagonizes inflammasome activation to the benefit of Mb

609 survival [65; 66]. In C57BL/6 mice treated with IFNAR1 blocking Ab and infected with

610 Mb, the recruitment of neutrophils was reduced but the pro-inflammatory profile of

611 MPs was increased, leading to reduced bacillary burden [67]. No impact on T-cells

612 was observed in this *in vivo* model, revealing a role of type I IFN signaling during the

613 innate phase of the host response to infection. Therefore, Mb exploits type I IFN

614 signaling in many ways and this pathway seems an important avenue to better

615 understand Mb virulence. The PCLS model will greatly help to better dissect out this

616 pathway in the lung during bTB. This could lead to new biomarkers to help genomic

617 selection programs for cattle that are more resistant to bTB, as well as new

618 immunostimulation strategies counteracting the type I IFN pathway. This new

619 knowledge will ultimately improve bTB control, a goal which is so greatly needed at

620 the global level [68].

621

635

636 **AUTHOR CONTRIBUTIONS**

637 AR designed and did most of the experiments, obtained funding, analyzed data,

638 prepared all figures and wrote the manuscript. NW obtained funding, supervised all

639 aspects of the work, critically analyzed the data and wrote the manuscript. FC

640 performed experiments and prepared the inocula for experimental infections under

641 BSL3 conditions. AC cultured AMPs, performed ELISA and q-RT-PCR. EDD helped

19

642 for PCLS experiments and revised the manuscript. MLB provided Mb3601 strain and

643 revised the manuscript. AA provided strain Mtb BTB1558. JAB improved the RNA

644 extraction protocol. DD and QM performed multiplex experiments. FA provided Ab

645 and critically reviewed imaging data. PG helped with transcriptomic analysis and

646 revised the manuscript. SVG obtained funding, designed experiments and revised

647 the manuscript. All authors read and approved the manuscript before publication.

648

649 **Competing Interests Statement**

650 The authors declare that the research was conducted in the absence of any

651 commercial or financial relationships that could be construed as a potential conflict of

652 interest

653

654 **Figure Legends**

655 **Figure 1: PCLS infection with four different Mb or Mtb strains does not induce**

656 **lung tissue cytotoxicity and equivalent numbers of bacilli are recovered 24 h**

657 **post-infection**

658 **(A)** PCLS prepared from Blonde d'Aquitaine lungs post-mortem were infected with

659 10^5 cfu of two Mb strains (AF2122 or Mb3601) or two Mtb strains (H37Rv or

660 BTB1558). After 1 and 2 days post infection, PCLS supernatants were harvested and

661 tissue was homogenized. Lactate deshydrogenase (LDH) was measured in both

662 compartments using the "Non-Radioactive Cytotoxicity Assay" kit. Cytotoxicity was

663 determined as (%) = (O.D.490nm LDH in supernatant) / (O.D.490nm LDH in

664 supernatant + O.D.490nm LDH in PCLS homogenates) x 100. Individual data and the

665 median and interquartile range in each group are presented (n=6 animals, from 6

666 independent experiments). **(B)** 24h post infection, PCLS were washed and

667 homogenized to recover bacilli. Inoculum and PCLS homogenates were serially

668 diluted and plated with CFUs numerated after 3-6 weeks incubation. Individual data

669 and the mean in each group are presented (n=6 independent inocula prepared,

670 PCLS homogenates data represent the mean of technical duplicates from n=3

671 animals, from 3 independent experiments).

672

673 **Figure 2: Mb3601 is internalized by AMPs in the preserved lung structure from**

674 **PCLS and infected alveoli contain higher numbers of AMPs as compared to**

675 **non-infected alveoli**

20

676   PCLS were infected with 10^5 CFUs of the green fluorescent Mb3601-GFP

677   recombinant strain and fixed 2 days later. After labelling with anti-pancytokeratine

678   (APC, magenta) and anti-MHCII antibodies (Alexa 555, red), PCLS were mounted

679   with Fluoromount-G™ Mounting Medium containing DAPI (blue) and analyzed under

680   a Leica confocal microscope **(A)**; 3D images were analyzed with Leica LAS

681   software. Z-stack imaging was performed at x63 enlargment (10-15µm of thickness,

682   step size of 0.5-1µm). White asterisks indicate extracellular bacilli and white arrows

683   indicate bacili inside MHC-II^{pos} AMPs. **(B)** Graph represents the percentage of

684   infected alveoli per PCLS among the 55 to 80 alveoli that were observed under the

685   microscope (n=4 PCLS from two different Blonde d'Aquitaine cattle) **(C)** Stack

686   histogram of the mean percentage +/- SEM of intra or extracellular bacilli among a

687   minimum of 15 infected alveoli that were observed (N=4 PCLS) **(D)** The number of

688   MHC-II^{pos} AMPs per alveoli was counted in infected or non-infected alveoli. The data

689   presented as % are the mean +/- SEM of n=4 PCLS from two different Blonde

690   d'Aquitaine cattle. Between 55 and 80 alveoli were observed to obtain these data

691   (two way ANOVA, *** $p<0.001$)

692

693   **Figure 3: Principal Component Analysis (PCA) of inflammatory lung tissue**

694   **signature reveals differences between two beef cattle breeds after 2 days of**

695   **infection by Mb or Mtb.**

696   **(A)** Fifteen cytokines and chemokines were measured in PCLS supernatants from

697   Blonde d'Aquitaine or Charolaise cows 2 days after infection with four different

698   mycobacterial strains. Raw data were used to run PCA in R studio. Individual data

699   are shown (n=4 for Charolaise, red; n=6 for Blonde d'Aquitaine, blue). Ellipses

700   represent a confidence range of 90%. **(B)** PCA were built from expression data of 96

701   genes ($2^{-\Delta\Delta Ct}$) obtained from PCLS total RNA extracted 2 days after infection.

702   Individual data are shown (n=9 for Charolaise, red; n=7 for Blonde d'Aquitaine, blue).

703   Ellipses represent a confidence range of 90%. **(C)** Two examples of differentially

704   expressed genes. Individual data and the median and interquartile range in each

705   group are presented (n=7 Blonde d'Aquitaine and n=9 Charolaise) * $p<0.05$. **

706     $p<0.01$. *** $p<0.001$. Two way ANOVA test.

707

708 **Figure 4: The lung inflammatory neutrophil and monocyte recruitment**
709 **signature induced by infection in PCLS from Blonde d'Aquitaine cows is more**
710 **efficiently triggered by *M. bovis* than *M. tuberculosis***

711 **(A)** Cytokine and chemokine levels were measured in PCLS supernatant by Multiplex
712 ELISA two days after infection with two Mb or two Mtb strains. Individual data and the
713 median and interquartile range in each group are presented (n=6 cows). **(B)** Table of
714 the mean of fold change (2^{-ddCT}) for each group (n=7 cows) of 17 major genes
715 involved in neutrophil and monocyte recruitment and inflammation. The graduated
716 red box coloring represents levels of gene expression, and asterisks mark significant
717 differences compared to non-infected controls. **(C)** *CXCL2*, *CXCL5* and *CXCL8* gene
718 expression at 2 days post infection. Individual data and the median and interquartile
719 range in each group are presented (n=7 cows). (B-C) * $p<0.05$ (Wilcoxon non
720 parametric test).

721

722 **Figure 5: Mb but not Mtb infection in the lung tissue from Blonde d'Aquitaine**
723 **cows induces the type I interferon pathway.**
724 PCLS were infected as described in Figure 1. **(A)** *IFNAR*, ISG15*, CXCL10* and *OAS1*
725 gene expression at 2 dpi. Individual data and the median and interquartile range in
726 each group are presented (n=7) **(B)** CXCL10 protein level was measured in PCLS
727 supernatant at 2 dpi. Individual data and the median and interquartile range in each
728 group are presented (n=6). **(C)** The table represents the mean of fold change (2^{-ddCT})
729 for each group (n=7) of major genes involved in type I interferon pathway. Graduated
730 red box coloring are for higher gene expression and asterisks mark significant
731 differences compared to uninfected PCLS. nd=not detected. **(D)** Ingenuity Pathway
732 Analysis drawing of the Type I interferon pathway under IFNAR in the Mb3601 group.
733 Graduated red box coloring are for higher gene expression. (A, B and C) * $p<0.05$
734 (Wilcoxon non parametric test).

735

736 **Figure 6: Alveolar macrophages from Blonde d'Aquitaine contribute to the type**
737 **I IFN signature in lung induced by Mb infection**
738 AMPs from Blonde d'Aquitaine lungs were infected with 10^5 cfu of Mb3601 or Mtb
739 H37Rv. 6 h later mRNA was extracted from and expression of major genes from the
740 type 1 IFN pathway was analyzed **(A)** Mean fold change (2^{-ddCT}) of gene expression
741 normalized to three house keeping genes was calculated in each group (n=7).

742 Graduated red box coloring represents gene expression and asterisks mark

743 significant differences compared to non infected controls (nd=not detected). **(B)**

744 *IFNβ*, *LPG2*, *RIG1*, *MX1* and *OAS1* gene expression in AMPs was analysed by RT-

745 qPCR at 6h post infection. Individual data and the median and interquartile range in

746 each group are presented (n=7). **(A, B)** * $p<0.05$ (Wilcoxon non parametric test).

747

748 **Figure 7: Superposition of Blonde d'Aquitaine and Charolaise beef breeds in**

749 **French counties where Mb outbreaks were declared between December 2019**

750 **and 2020.**

751 This map of France shows counties where Mb outbreaks were declared between

752 December 2019 and December 2020 (yellow stars) and was obtained with data

753 extracted from https://www.plateforme-esa.fr/. Herd densities of Blonde d'Aquitaine

754 (blue), Charolaise (red) or both breeds (violet) were extracted from data obtained

755 from https://www.racesdefrance.fr (cows above 3-years-old have been considered).

756

757 **Supplementary table and figures legends**

758

759 **Supplementary Table S1. Sequences of primers used in this study.**

760 Primers were designed using Geneious software, in intron-spanning regions when

761 possible. The annealing temperature was set at 60°C. Housekeeping genes used as

762 the reference to calculate ΔCT are indicated in the grey boxes.

763

764 **Figure S1: Age and geographical origin of cows used in the study**

765 The Charolaise and Blonde d'Aquitaine cows used were between 3- to 11-years-old,

766 and came from 8 different French departments. Two Blonde d'Aquitaine cows came

767 from the same farm in Indre et Loire; et three Charolaise cows from the same farm in

768 Sarthe. All other animals are from distinct farms. Data represent the age of individual

769 animal and the median and interquartile range.

770

771 **Figure S2: Transcriptomic signature after infection with different doses of**

772 **mycobacteria**

773 Bovine PCLS were obtained as described in Fig. 1 and infected with 10^5, 5×10^5, 10^6

774 or 5×10^6 cfu. RNA were extracted 2 dpi after infection and *SDC4*, *CXCL1*, *HIF1* and

775 *OAS1* gene expression were assessed with the Fluidigm Biomark. Individual data

23

776 and the mean and standard deviation in each group are presented (n=3 Charolaise).

777 The dotted line represent the level of expression in the uninfected group.

778

779 **Figure S3: Cytokines/Chemokines in PCLS supernatants.**

780 Protein levels were measured in PCLS supernatant at 2 dpi post infection with

781 Multiplex. Individual data and the median and interquartile range in each group are

782 presented (n=6). * $p<0.05$ (Wilcoxon non parametric test).

783

784 **Figure S4: Structure of bovine PCLS under light microscope.**

785 PCLS were observed under a light microscope (enlargement x40 to x200). PCLS

786 contain numerous alveoli and between one to three bronchioles, with thick and wavy

787 epithelium that can be easily recognized (black asterisk). Thin blood vessels (red

788 dotted lines) were localised next to bronchioles and diffused between alveoli. No

789 blood cells remained inside the endothelium (cows were bled out at the abattoir).

790 Alveolar macrophages can be seen inside alveoli (black arrows).

791

792 **Supplementary video 1: Internalisation of Mb3601 in alveolar macrophages**

793 **after PCLS *ex vivo* infection.**

794 PCLS were fixed at 2 dpi with 10^5 cfu of Mb3601-GFP recombinant strain, and

795 labeled with anti-pancytokeratine and anti-MHCII antibodies, respectively revealed

796 with APC, and Alexa 555 conjugated secondary Ab. PCLS were transferred on

797 coverslides and mounted with Fluoromount-G™ Mounting Medium, containing DAPI.

798 Z-stack imaging was performed at x63 enlargment with a confocal microscope. 3D

799 images were analyzed with Leica LAS software.

800

801 **REFERENCES**

802 [1] S.H. Downs, A. Prosser, A. Ashton, S. Ashfield, L.A. Brunton, A. Brouwer, P. Upton, A.
803 Robertson, C.A. Donnelly, and J.E. Parry, Assessing effects from four years of
804 industry-led badger culling in England on the incidence of bovine tuberculosis in
805 cattle, 2013-2017. Sci Rep 9 (2019) 14666.
806 [2] A. Pereira, A. Reis, B. Ramos, and M. Cunha, Animal tuberculosis: Impact of disease
807 heterogeneity in transmission, diagnosis and control. Transbound Emerg Dis (2020).
808 [3] A. Hauer, K. De Cruz, T. Cochard, S. Godreuil, C. Karoui, S. Henault, T. Bulach, A.L.
809 Banuls, F. Biet, and M.L. Boschiroli, Genetic evolution of Mycobacterium bovis
810 causing tuberculosis in livestock and wildlife in France since 1978. PLoS One 10
811 (2015) e0117103.
812 [4] E. Reveillaud, S. Desvaux, M.L. Boschiroli, J. Hars, E. Faure, A. Fediaevsky, L. Cavalerie,
813 F. Chevalier, P. Jabert, S. Poliak, I. Tourette, P. Hendrikx, and C. Richomme,

814   Infection of Wildlife by Mycobacterium bovis in France Assessment Through a
815   National Surveillance System, Sylvatub. Front Vet Sci 5 (2018) 262.
816 [5] E. Harding, WHO global progress report on tuberculosis elimination. Lancet Respir Med 8
817   (2020) 19.
818 [6] S. Cole, R. Brosch, J. Parkhill, T. Garnier, C. Churcher, D. Harris, S. Gordon, K.
819   Eiglmeier, Gas S, Barry CE 3rd, Tekaia F, Badcock K, Basham D, Brown D,
820   Chillingworth T, Connor R, Davies R, Devlin K, Feltwell T, Gentles S, Hamlin N,
821   Holroyd S, Hornsby T, Jagels K, Krogh A, McLean J, Moule S, Murphy L, Oliver K,
822   Osborne J, Quail MA, Rajandream MA, Rogers J, Rutter S, Seeger K, Skelton J,
823   Squares R, Squares S, Sulston JE, Taylor K, S. Whitehead, and B. Barrell,
824   Deciphering the biology of Mycobacterium tuberculosis from the complete genome
825   sequence. Nature 393 (1998) 537-44.
826 [7] A.O. Whelan, M. Coad, P.J. Cockle, G. Hewinson, M. Vordermeier, and S.V. Gordon,
827   Revisiting host preference in the Mycobacterium tuberculosis complex: experimental
828   infection shows M. tuberculosis H37Rv to be avirulent in cattle. PLoS One 5 (2010)
829   e8527.
830 [8] D.A. Magee, K. Conlon, N.C. Nalpas, J.A. Browne, C. Pirson, C. Healy, K.E. McLoughlin,
831   J. Chen, M.H. Vordermeier, E. Gormley, D. MacHugh, and S. Gordon, Innate cytokine
832   profiling of bovine alveolar macrophages reveals commonalities and divergence in
833   the response to Mycobacterium bovis and Mycobacterium tuberculosis infection.
834   Tuberculosis (Edinb) 94 (2014) 441-50.
835 [9] G. Ameni, M. Vordermeier, R. Firdessa, A. Aseffa, G. Hewinson, S.V. Gordon, and S.
836   Berg, Mycobacterium tuberculosis infection in grazing cattle in central Ethiopia. Vet J
837   188 (2011) 359-61.
838 [10] J.M. van den Berg, E. van Koppen, A. Ahlin, B.H. Belohradsky, E. Bernatowska, L.
839   Corbeel, T. Espanol, A. Fischer, M. Kurenko-Deptuch, R. Mouy, T. Petropoulou, J.
840   Roesler, R. Seger, M.J. Stasia, N.H. Valerius, R.S. Weening, B. Wolach, D. Roos,
841   and T.W. Kuijpers, Chronic granulomatous disease: the European experience. PLoS
842   One 4 (2009) e5234.
843 [11] T. Garnier, K. Eiglmeier, J.C. Camus, N. Medina, H. Mansoor, M. Pryor, S. Duthoy, S.
844   Grondin, C. Lacroix, C. Monsempe, S. Simon, B. Harris, R. Atkin, J. Doggett, R.
845   Mayes, L. Keating, P.R. Wheeler, J. Parkhill, B.G. Barrell, S.T. Cole, S.V. Gordon,
846   and R.G. Hewinson, The complete genome sequence of Mycobacterium bovis. Proc
847   Natl Acad Sci U S A 100 (2003) 7877-82.
848 [12] K.M. Malone, D. Farrell, T.P. Stuber, O.T. Schubert, R. Aebersold, S. Robbe-Austerman,
849   and S.V. Gordon, Updated Reference Genome Sequence and Annotation of
850   Mycobacterium bovis AF2122/97. Genome Announc 5 (2017).
851 [13] B. Villarreal-Ramos, S. Berg, A. Whelan, S. Holbert, F. Carreras, F.J. Salguero, B.L.
852   Khatri, K. Malone, K. Rue-Albrecht, R. Shaughnessy, A. Smyth, G. Ameni, A. Aseffa,
853   P. Sarradin, N. Winter, M. Vordermeier, and S.V. Gordon, Experimental infection of
854   cattle with Mycobacterium tuberculosis isolates shows the attenuation of the human
855   tubercle bacillus for cattle. Sci Rep 8 (2018) 894.
856 [14] N. Smith, S. Berg, J. Dale, A. Allen, S. Rodriguez, B. Romero, F. Matos, S.
857   Ghebremichael, D.C. Karoui C, Machado Ada C, Mucavele C, Kazwala RR, Hilty M,
858   Cadmus S, Ngandolo BN, Habtamu M, Oloya J, Muller A, Milian-Suazo F,
859   Andrievskaia O, Projahn M, Barandiarán S, Macías A, Müller B, Zanini MS, Ikuta CY,
860   Rodriguez CA, Pinheiro SR, Figueroa A, Cho SN, Mosavari N, Chuang PC, Jou R,
861   Zinsstag J, van Soolingen D, Costello E, Aseffa A, Proaño-Perez F, Portaels F,
862   Rigouts L, Cataldi AA, Collins DM, Boschiroli ML, Hewinson RG, Ferreira Neto JS,
863   Surujballi O, Tadyon K, Botelho A, Zárraga AM, Buller N, Skuce R, Michel A, Aranaz
864   A, , S. Gordon, B. Jeon, G. Källenius, S. Niemann, M. Boniotti, P. van Helden, B.
865   Harris, M. Zumárraga, and K. Kremer, European 1: a globally important clonal
866   complex of Mycobacterium bovis. Infect Genet Evol 11 (2011) 1340-51.

867 [15] M. Branger, V. Loux, T. Cochard, M. Boschiroli, F. Biet, and L. Michelet, The complete
868   genome sequence of Mycobacterium bovis Mb3601, a SB0120 spoligotype strain
869   representative of a new clonal group. Infect Genet Evol 82 (2020).
870 [16] A. Hauer, L. Michelet, T. Cochard, M. Branger, J. Nunez, M.L. Boschiroli, and F. Biet,
871   Accurate Phylogenetic Relationships Among Mycobacterium bovis Strains Circulating
872   in France Based on Whole Genome Sequencing and Single Nucleotide
873   Polymorphism Analysis. Front Microbiol 10 (2019) 955.
874 [17] R. Brosch, S.V. Gordon, T. Garnier, K. Eiglmeier, W. Frigui, P. Valenti, S. Dos Santos,
875   S. Duthoy, C. Lacroix, C. Garcia-Pelayo, J.K. Inwald, P. Golby, J.N. Garcia, R.G.
876   Hewinson, M.A. Behr, M.A. Quail, C. Churcher, B.G. Barrell, J. Parkhill, and S.T.
877   Cole, Genome plasticity of BCG and impact on vaccine efficacy. Proc Natl Acad Sci U
878   S A 104 (2007) 5596-601.
879 [18] C. Cosma, O. Humbert, and L. Ramakrishnan, Superinfecting mycobacteria home to
880   established tuberculous granulomas. Nature Immunology 5 (2004) 828-35.
881 [19] J. Cassidy, The pathogenesis and pathology of bovine tuberculosis with insights from
882   studies of tuberculosis in humans and laboratory animal models. Veterinary
883   Microbiology 112 (2006) 151-61.
884 [20] J.M. Scordo, D.L. Knoell, and J.B. Torrelles, Alveolar Epithelial Cells in Mycobacterium
885   tuberculosis Infection: Active Players or Innocent Bystanders? J Innate Immun 8
886   (2016) 3-14.
887 [21] Y. Li, Y. Wang, and X. Liu, The role of airway epithelial cells in response to mycobacteria
888   infection. Clin Dev Immunol 2012 (2012) 791392.
889 [22] M.B. Ryndak, and S. Laal, Mycobacterium tuberculosis Primary Infection and
890   Dissemination: A Critical Role for Alveolar Epithelial Cells. Front Cell Infect Microbiol
891   9 (2019) 299.
892 [23] V.V. Thacker, N. Dhar, K. Sharma, R. Barrile, K. Karalis, and J.D. McKinney, A lung-on-
893   chip model of early Mycobacterium tuberculosis infection reveals an essential role for
894   alveolar epithelial cells in controlling bacterial growth. Elife 9 (2020).
895 [24] K. Sato, H. Tomioka, T. Shimizu, T. Gonda, F. Ota, and C. Sano, Type II alveolar cells
896   play roles in macrophage-mediated host innate resistance to pulmonary
897   mycobacterial infections by producing proinflammatory cytokines. Journal of
898   Infectious Disease 185 (2002) 1139-47.
899 [25] D.F. Lee, G.R. Stewart, and M.A. Chambers, Modelling early events in Mycobacterium
900   bovis infection using a co-culture model of the bovine alveolus. Sci Rep 10 (2020)
901   18495.
902 [26] K. Goris, S. Uhlenbruck, C. Schwegmann-Wessels, W. Kohl, F. Niedorf, M. Stern, M.
903   Hewicker-Trautwein, R. Bals, G. Taylor, A. Braun, G. Bicker, M. Kietzmann, and G.
904   Herrler, Differential sensitivity of differentiated epithelial cells to respiratory viruses
905   reveals different viral strategies of host infection. J Virol 83 (2009) 1962-8.
906 [27] Q. Marquant, D. Laubreton, C. Drajac, E. Mathieu, E. Bouguyon, M.L. Noordine, A.
907   Remot, S. Riffault, M. Thomas, and D. Descamps, The microbiota plays a critical role
908   in the reactivity of lung immune components to innate ligands. FASEB J 35 (2021)
909   e21348.
910 [28] P. Carranza-Rosales, I.E. Carranza-Torres, N.E. Guzman-Delgado, G. Lozano-Garza, L.
911   Villarreal-Trevino, C. Molina-Torres, J.V. Villarreal, L. Vera-Cabrera, and J. Castro-
912   Garza, Modeling tuberculosis pathogenesis through ex vivo lung tissue infection.
913   Tuberculosis (Edinb) 107 (2017) 126-132.
914 [29] K.J. Bryson, D. Garrido, M. Esposito, G. McLachlan, P. Digard, C. Schouler, R.
915   Guabiraba, S. Trapp, and L. Vervelde, Precision cut lung slices: a novel versatile tool
916   to examine host-pathogen interaction in the chicken lung. Vet Res 51 (2020) 2.
917 [30] T. Thacker, M. Palmer, and W. Waters, Associations between cytokine gene expression
918   and pathology in Mycobacterium bovis infected cattle. Veterinary Immunology and
919   Immunopathology 119 (2007) 204-13.
920 [31] K.M. Malone, K. Rue-Albrecht, D.A. Magee, K. Conlon, O.T. Schubert, N.C. Nalpas, J.A.
921   Browne, A. Smyth, E. Gormley, R. Aebersold, D.E. MacHugh, and S.V. Gordon,

922   Comparative 'omics analyses differentiate Mycobacterium tuberculosis and
923   Mycobacterium bovis and reveal distinct macrophage responses to infection with the
924   human and bovine tubercle bacilli. Microb Genom 4 (2018).

925 [32] A.R. Allen, G. Minozzi, E.J. Glass, R.A. Skuce, S.W. McDowell, J.A. Woolliams, and
926   S.C. Bishop, Bovine tuberculosis: the genetic basis of host susceptibility. Proc Biol
927   Sci 277 (2010) 2737-45.

928 [33] V. Abadie, E. Badell, P. Douillard, D. Ensergueix, P.J. Leenen, M. Tanguy, L. Fiette, S.
929   Saeland, B. Gicquel, and N. Winter, Neutrophils rapidly migrate via lymphatics after
930   Mycobacterium bovis BCG intradermal vaccination and shuttle live bacilli to the
931   draining lymph nodes. Blood 106 (2005) 1843-50.

932 [34] M.P.R. Berry, C.M. Graham, F.W. McNab, Z. Xu, S.A.A. Bloch, T. Oni, K.A. Wilkinson,
933   R. Banchereau, R.J.W. Jason Skinner, Charles Quinn, Derek Blankenship, Ranju
934   Dhawan, John J. Cush, Asuncion Mejias, Octavio Ramilo, Onn M. Kon, Virginia
935   Pascual, , J. Banchereau, D. Chaussabel, and A. O'Garra, An Interferon-Inducible
936   Neutrophil-Driven Blood Transcriptional Signature in Human Tuberculosis. Nature
937   466 (2010) 973-977.

938 [35] L. Moreira-Teixeira, K. Mayer-Barber, A. Sher, and A. O'Garra, Type I interferons in
939   tuberculosis: Foe and occasionally friend. J Exp Med 215 (2018) 1273-1285.

940 [36] D.X. Ji, L.H. Yamashiro, K.J. Chen, N. Mukaida, I. Kramnik, K.H. Darwin, and R.E.
941   Vance, Type I interferon-driven susceptibility to Mycobacterium tuberculosis is
942   mediated by IL-1Ra. Nat Microbiol 4 (2019) 2128-2135.

943 [37] F. Menzies, and S. Neill, Cattle-to-cattle transmission of bovine tuberculosis. Veterinary
944   Journal 160 (2000) 92-106.

945 [38] A. Neupane, M. Willson, A. Krzysztof Chojnacki, F. Vargas E Silva Castanheira, C.
946   Morehouse, A. Carestia, A. Keller, M. Peiseler, A. DiGiandomenico, M. Kelly, M.
947   Amrein, C. Jenne, A. Thanabalasuriar, and P. Kubes, Patrolling Alveolar
948   Macrophages Conceal Bacteria from the Immune System to Maintain Homeostasis.
949   Cell 183 (2020) 110-125.

950 [39] C.J. Queval, R. Brosch, and R. Simeone, The Macrophage: A Disputed Fortress in the
951   Battle against Mycobacterium tuberculosis. Front Microbiol 8 (2017) 2284.

952 [40] D. Wedlock, R. Kawakami, J. Koach, B. Buddle, and D. Collins, Differences of gene
953   expression in bovine alveolar macrophages infected with virulent and attenuated
954   isogenic strains of Mycobacterium bovis. Int Immunopharmacol 6 (2006) 957-61.

955 [41] C.J. Queval, A. Fearns, L. Botella, A. Smyth, L. Schnettger, M. Mitermite, E. Wooff, B.
956   Villarreal-Ramos, W. Garcia-Jimenez, T. Heunis, M. Trost, D. Werling, F.J. Salguero,
957   S.V. Gordon, and M.G. Gutierrez, Macrophage-specific responses to human- and
958   animal-adapted tubercle bacilli reveal pathogen and host factors driving
959   multinucleated cell formation. PLoS Pathog 17 (2021) e1009410.

960 [42] J. Ferguson, and L. Schlesinger, Pulmonary surfactant in innate immunity and the
961   pathogenesis of tuberculosis. Tuberculosis Lung Disease 80 (2000) 173-84.

962 [43] J. Cassidy, and A. Martineau, Innate resistance to tuberculosis in man, cattle and
963   laboratory animal models: nipping disease in the bud? Comparative Pathology 151
964   (2014) 291-308.

965 [44] M.V. Palmer, J. Wiarda, C. Kanipe, and T.C. Thacker, Early Pulmonary Lesions in Cattle
966   Infected via Aerosolized Mycobacterium bovis. Vet Pathol 56 (2019) 544-554.

967 [45] A.R. Martineau, S.M. Newton, K.A. Wilkinson, B. Kampmann, B.M. Hall, N. Nawroly,
968   G.E. Packe, R.N. Davidson, C.J. Griffiths, and R.J. Wilkinson, Neutrophil-mediated
969   innate immune resistance to mycobacteria. J Clin Invest 117 (2007) 1988-94.

970 [46] T. McCorry, A. Whelan, M. Welsh, J. McNair, E. Walton, D. Bryson, R. Hewinson, H.
971   Vordermeier, and J. Pollock, Shedding of Mycobacterium bovis in the nasal mucus of
972   cattle infected experimentally with tuberculosis by the intranasal and intratracheal
973   routes. Veterinary Record 157 (2005) 613-8.

974 [47] F. Su, X. Liu, G. Liu, Y. Yu, Y. Wang, Y. Jin, G. Hu, S. Hua, and Y. Zhang,
975   Establishment and evaluation of a stable cattle type II alveolar epithelial cell line.
976   PLoS One 8 (2013) e76036.

977   [48] G. Ameni, A. Aseffa, H. Engers, D. Young, S. Gordon, G. Hewinson, and M.
978   Vordermeier, High prevalence and increased severity of pathology of bovine
979   tuberculosis in Holsteins compared to zebu breeds under field cattle husbandry in
980   central Ethiopia. Clin Vaccine Immunol 14 (2007) 1356-61.

981   [49] U. Castillo-Velázquez, R. Gomez-Flores, R. Tamez-Guerra, P. Tamez-Guerra, and C.
982   Rodríguez-Padilla, Differential responses of macrophages from bovines naturally
983   resistant or susceptible to Mycobacterium bovis after classical and alternative
984   activation. Veterinary Immunology and Immunopathology 154 (2013) 8-16.

985   [50] K. Raphaka, E. Sanchez-Molano, S. Tsairidou, O. Anacleto, E.J. Glass, J.A. Woolliams,
986   A. Doeschl-Wilson, and G. Banos, Impact of Genetic Selection for Increased Cattle
987   Resistance to Bovine Tuberculosis on Disease Transmission Dynamics. Front Vet Sci
988   5 (2018) 237.

989   [51] G. Banos, M. Winters, R. Mrode, A.P. Mitchell, S.C. Bishop, J.A. Woolliams, and M.P.
990   Coffey, Genetic evaluation for bovine tuberculosis resistance in dairy cattle. J Dairy
991   Sci 100 (2017) 1272-1281.

992   [52] K. Raphaka, O. Matika, E. Sanchez-Molano, R. Mrode, M.P. Coffey, V. Riggio, E.J.
993   Glass, J.A. Woolliams, S.C. Bishop, and G. Banos, Genomic regions underlying
994   susceptibility to bovine tuberculosis in Holstein-Friesian cattle. BMC Genet 18 (2017)
995   27.

996   [53] I.W. Richardson, D.P. Berry, H.L. Wiencko, I.M. Higgins, S.J. More, J. McClure, D.J.
997   Lynn, and D.G. Bradley, A genome-wide association study for genetic susceptibility to
998   Mycobacterium bovis infection in dairy cattle identifies a susceptibility QTL on
999   chromosome 23. Genet Sel Evol 48 (2016) 19.

1000   [54] S.C. Ring, D.C. Purfield, M. Good, P. Breslin, E. Ryan, A. Blom, R.D. Evans, M.L.
1001   Doherty, D.G. Bradley, and D.P. Berry, Variance components for bovine tuberculosis
1002   infection and multi-breed genome-wide association analysis using imputed whole
1003   genome sequence data. PLoS One 14 (2019) e0212067.

1004   [55] S. Wilkinson, S.C. Bishop, A.R. Allen, S.H. McBride, R.A. Skuce, M. Bermingham, J.A.
1005   Woolliams, and E.J. Glass, Fine-mapping host genetic variation underlying outcomes
1006   to Mycobacterium bovis infection in dairy cows. BMC Genomics 18 (2017) 477.

1007   [56] L. Abel, J. Fellay, D.W. Haas, E. Schurr, G. Srikrishna, M. Urbanowski, N. Chaturvedi, S.
1008   Srinivasan, D. Johnson, and W. Bishai, Genetics of human susceptibility to active and
1009   latent tuberculosis: present knowledge and future perspectives. Lancet Infect Dis 18
1010   (2018) e64-e75.

1011   [57] A. Allen, One bacillus to rule them all? - Investigating broad range host adaptation in
1012   Mycobacterium bovis. Infect Genet Evol 53 (2017) 68-76.

1013   [58] J. Sabio Y García, M.M. Bigi, L.I. Klepp, E.A. García, F.F. Blanco, and F. Bigi, Does
1014   Mycobacterium bovis persist in cattle in a non-replicative latent state as
1015   Mycobacterium tuberculosis in human beings? Vet Microbiol 247 (2020).

1016   [59] J. Gonzalo-Asensio, W. Malaga, A. Pawlik, C. Astarie-Dequeker, C. Passemar, F.
1017   Moreau, F. Laval, M. Daffe, C. Martin, R. Brosch, and C. Guilhot, Evolutionary history
1018   of tuberculosis shaped by conserved mutations in the PhoPR virulence regulator.
1019   Proc Natl Acad Sci U S A 111 (2014) 11491-6.

1020   [60] K. Huynh, S. Joshi, and E. Brown, A delicate dance: host response to mycobacteria.
1021   Current Opinion in Immunology 23 (2011) 464-72.

1022   [61] D.G. Russell, Mycobacterium tuberculosis and the intimate discourse of a chronic
1023   infection. Immunol Rev 240 (2011) 252-68.

1024   [62] N.C. Nalpas, D.A. Magee, K.M. Conlon, J.A. Browne, C. Healy, K.E. McLoughlin, K.
1025   Rue-Albrecht, P.A. McGettigan, K.E. Killick, E. Gormley, S.V. Gordon, and D.E.
1026   MacHugh, RNA sequencing provides exquisite insight into the manipulation of the
1027   alveolar macrophage by tubercle bacilli. Sci Rep 5 (2015) 13629.

1028   [63] K. Jensen, I.J. Gallagher, N. Johnston, M. Welsh, R. Skuce, J.L. Williams, and E.J.
1029   Glass, Variation in the Early Host-Pathogen Interaction of Bovine Macrophages with
1030   Divergent Mycobacterium bovis Strains in the United Kingdom. Infect Immun 86
1031   (2018).

1032 [64] M. Palmer, T. Thacker, M. Rabideau, G. Jones, C. Kanipe, H. Vordermeier, and W.
1033   Waters, Biomarkers of cell-mediated immunity to bovine tuberculosis. Veterinary
1034   Immunology and Immunopathology 220 (2020).
1035 [65] L. Chunfa, S. Xin, L. Qiang, S. Sreevatsan, L. Yang, D. Zhao, and X. Zhou, The Central
1036   Role of IFI204 in IFN-beta Release and Autophagy Activation during Mycobacterium
1037   bovis Infection. Front Cell Infect Microbiol 7 (2017) 169.
1038 [66] C. Liu, E. Yue, Y. Yang, Y. Cui, L. Yang, D. Zhao, and X. Zhou, AIM2 inhibits autophagy
1039   and IFN-β production during M. bovis infection. Oncotarget 7 (2016) 46972-46987.
1040 [67] J. Wang, T. Hussain, K. Zhang, Y. Liao, J. Yao, Y. Song, N. Sabir, G. Cheng, H. Dong,
1041   M. Li, J. Ni, M.H. Mangi, D. Zhao, and X. Zhou, Inhibition of type I interferon signaling
1042   abrogates early Mycobacterium bovis infection. BMC Infect Dis 19 (2019) 1031.
1043 [68] F. Olea-Popelka, A. Muwonge, A. Perera, A. Dean, E. Mumford, E. Erlacher-Vindel, S.
1044   Forcella, B. Silk, L. Ditiu, A. El Idrissi, M. Raviglione, O. Cosivi, P. LoBue, and P.
1045   Fujiwara, Zoonotic tuberculosis in human beings caused by Mycobacterium bovis-a
1046   call for action. Lancet Infect Dis 17 (2017) e21-e25.
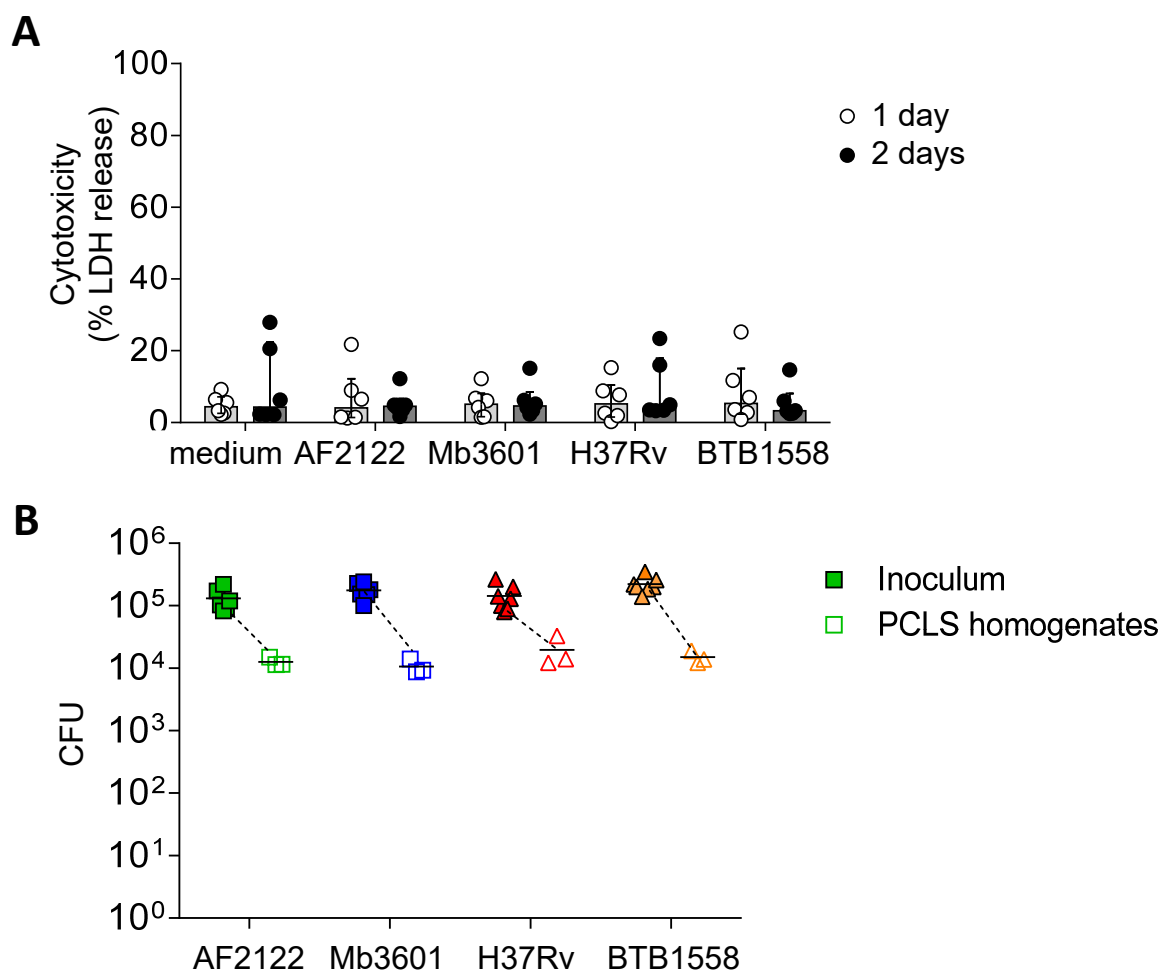1047

Figure 1: PCLS infection with four different Mb or Mtb strains does not induce lung tissue cytotoxicity and equivalent numbers of bacilli are recovered 24 h post-infection

(A) PCLS prepared from Blonde d'Aquitaine lungs post-mortem were infected with 10^5 cfu of two Mb strains (AF2122 or Mb3601) or two Mtb strains (H37Rv or BTB1558). After 1 and 2 days post infection, PCLS supernatants were harvested and tissue was homogenized. Lactate deshydrogenase (LDH) was measured in both compartments using the "Non-Radioactive Cytotoxicity Assay" kit. Cytotoxicity was determined as (%) = (O.D.490nm LDH in supernatant) / (O.D.490nm LDH in supernatant + O.D.490nm LDH in PCLS homogenates) x 100. Individual data and the median and interquartile range in each group are presented (n=6 animals, from 6 independent experiments). (B) 24h post infection, PCLS were washed and homogenized to recover bacilli. Inoculum and PCLS homogenates were serially diluted and plated with CFUs numerated after 3-6 weeks incubation. Individual data and the mean in each group are presented (n=6 independent inocula prepared, PCLS homogenates data represent the mean of technical duplicates from n=3 animals, from 3 independent experiments).

A.

- DAPI
- Mb3601-GFP
- MHCII A555
- Pancytokeratine APC

B. % of infected alveoli

C. Localisation of Mb3601-GFP (%) — Inside macrophage / Outside macrophage

D. Number of macrophages / alveoli — ≥ 4 / 2 or 3 / 1 / 0 — no / yes — Mb3601 in alveoli — ***
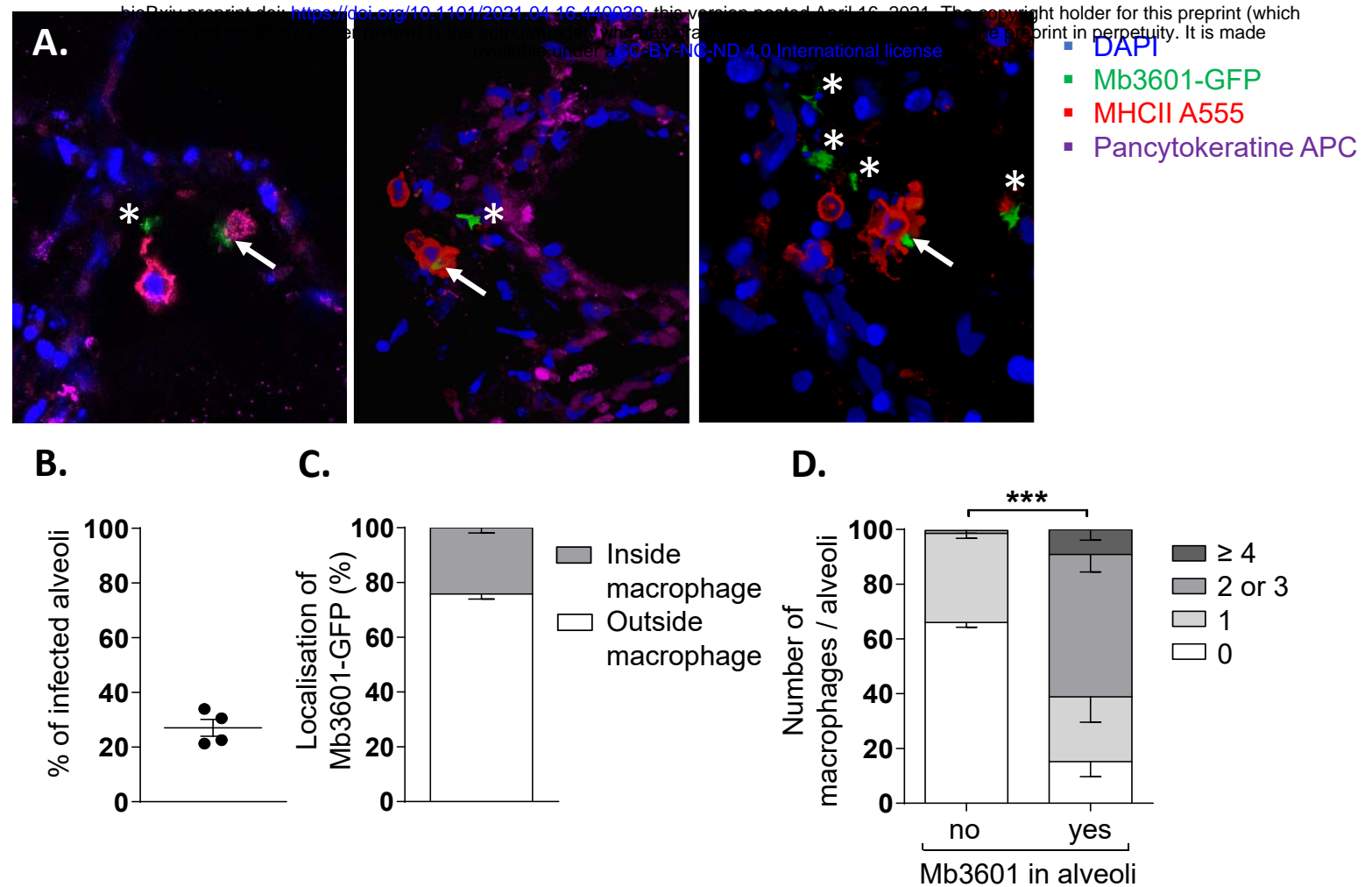
Figure 2: Mb3601 is internalized by AMPs in the preserved lung structure from PCLS and infected alveoli contain higher numbers of AMPs as compared to non-infected alveoli

PCLS were infected with 10^5 CFUs of the green fluorescent Mb3601-GFP recombinant strain and fixed 2 days later. After labelling with anti-pancytokeratine (APC, magenta) and anti-MHCII antibodies (Alexa 555, red), PCLS were mounted with Fluoromount-G™ Mounting Medium containing DAPI (blue) and analyzed under a Leica confocal microscope **(A)**; 3D images were analyzed with Leica LAS software. Z-stack imaging was performed at x63 enlargment (10-15µm of thickness, step size of 0.5-1µm). White asterisks indicate extracellular bacilli and white arrows indicate bacili inside MHC-II[pos] AMPs. **(B)** Graph represents the percentage of infected alveoli per PCLS among the 55 to 80 alveoli that were observed under the microscope (n=4 PCLS from two different Blonde d'Aquitaine cattle) **(C)** Stack histogram of the mean percentage +/- SEM of intra or extracellular bacilli among a minimum of 15 infected alveoli that were observed (N=4 PCLS) **(D)** The number of MHC-II[pos] AMPs per alveoli was counted in infected or non-infected alveoli. The data presented as % are the mean +/- SEM of n=4 PCLS from two different Blonde d'Aquitaine cattle. Between 55 and 80 alveoli were observed to obtain these data (two way ANOVA, *** $p<0.001$)
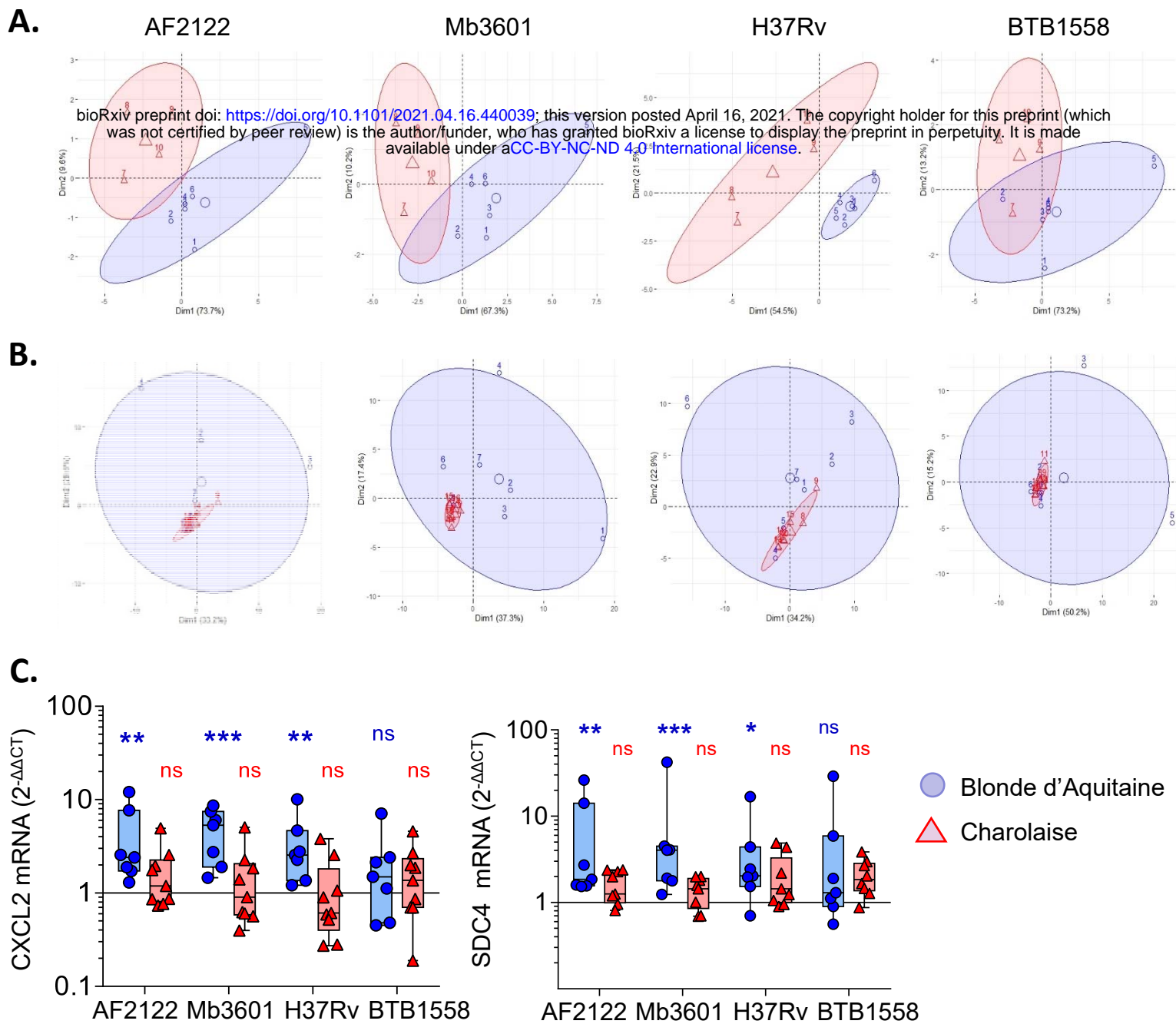
Figure 3: Principal Component Analysis (PCA) of inflammatory lung tissue signature reveals differences between two beef cattle breeds after 2 days of infection by Mb or Mtb.

(A) Fifteen cytokines and chemokines were measured in PCLS supernatants from Blonde d'Aquitaine or Charolaise cows 2 days after infection with four different mycobacterial strains. Raw data were used to run PCA in R studio. Individual data are shown (n=4 for Charolaise, red; n=6 for Blonde d'Aquitaine, blue). Ellipses represent a confidence range of 90%. **(B)** PCA were built from expression data of 96 genes ($2^{-\Delta\Delta Ct}$) obtained from PCLS total RNA extracted 2 days after infection. Individual data are shown (n=9 for Charolaise, red; n=7 for Blonde d'Aquitaine, blue). Ellipses represent a confidence range of 90%. **(C)** Two examples of differentially expressed genes. Individual data and the median and interquartile range in each group are presented (n=7 Blonde d'Aquitaine and n=9 Charolaise) * $p<0.05$. ** $p<0.01$. *** $p<0.001$. Two way ANOVA test.
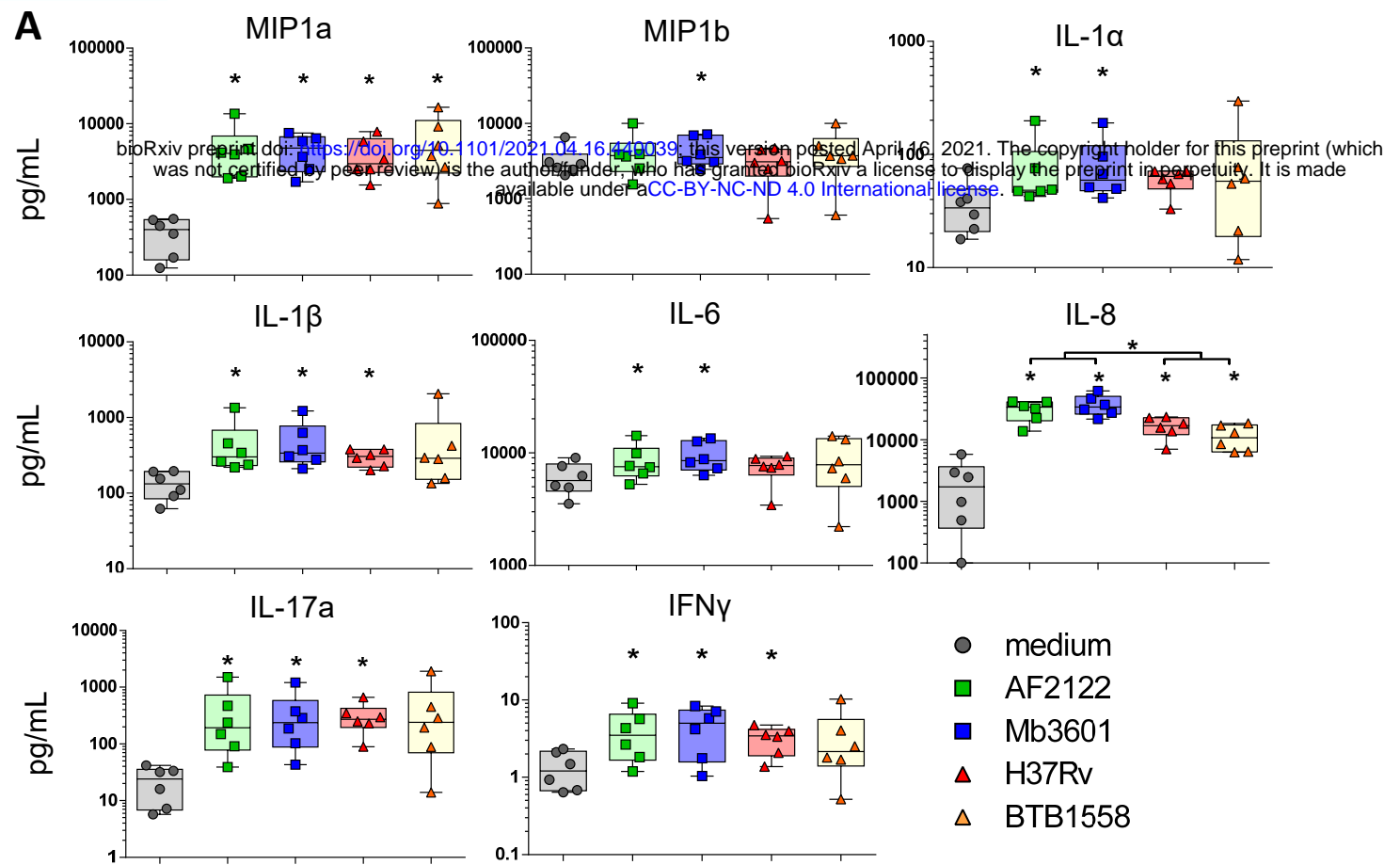
B

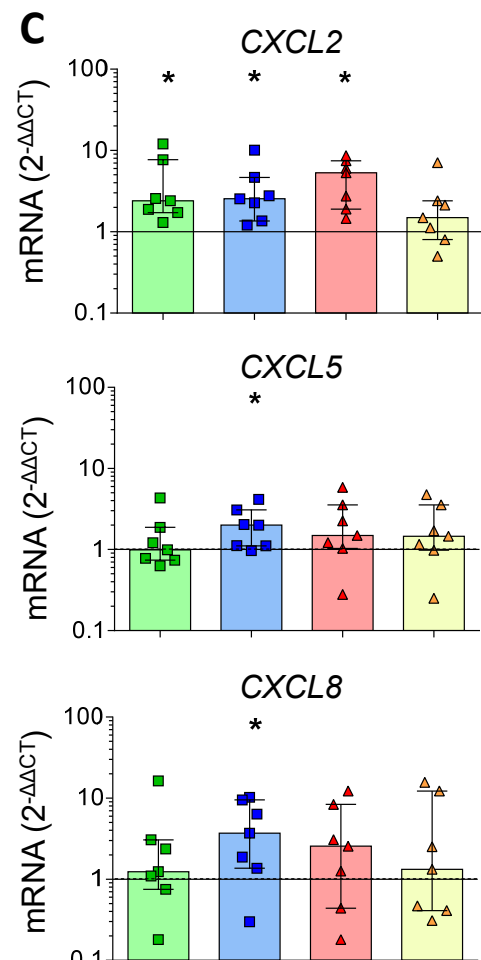| Gene ID	AF2122	Mb3601	H37Rv	BTB1558
IL-1α	1.7	3.8	2.7	2.2
IL-1β	1.9	4.1	2.5	3.4
IL-6	4,2	**7.3 ***	4.2	4.5
IL-17a	4.5	10.9	2.3	2.1
CCL2	4.2	7.1	2.4	6.3
CCL5	3.9	5.5	6.4	5.5
CCL20	4.4	2.0	5.8	4.1
CXCL1	3.2	**4.2 ***	3.3	3.0
CXCL2	**4.2 ***	**3.6 ***	**4.8 ***	2.2
CXCL5	1.5	**2.1 ***	2.2	2.0
CXCL8	3.6	**4.8 ***	4.0	4.7
G-CSF	**21.1 ***	1.7	8.3	3.9
GM-CSF	3	1.5	4.3	7.5
MIF	3.2	2.8	3.9	3.3
S100A8	5.5	7.5	3.1	6.7
S100A9	1.7	2.4	1.8	1.5
TNFα	16.4	14.1	2.4	3.7

Figure 4: The lung inflammatory neutrophil and monocyte recruitment signature induced by infection in PCLS from Blonde d'Aquitaine cows is more efficiently triggered by *M. bovis* than *M. tuberculosis*

(A) Cytokine and chemokine levels were measured in PCLS supernatant by Multiplex ELISA two days after infection with two Mb or two Mtb strains. Individual data and the median and interquartile range in each group are presented (n=6 cows). **(B)** Table of the mean of fold change (2^{-ddCT}) for each group (n=7 cows) of 17 major genes involved in neutrophil and monocyte recruitment and inflammation. The graduated red box coloring represents levels of gene expression, and asterisks mark significant differences compared to non-infected controls. **(C)** *CXCL2*, *CXCL5* and *CXCL8* gene expression at 2 days post infection. Individual data and the median and interquartile range in each group are presented (n=7 cows). (B-C) * $p < 0.05$ (Wilcoxon non parametric test).
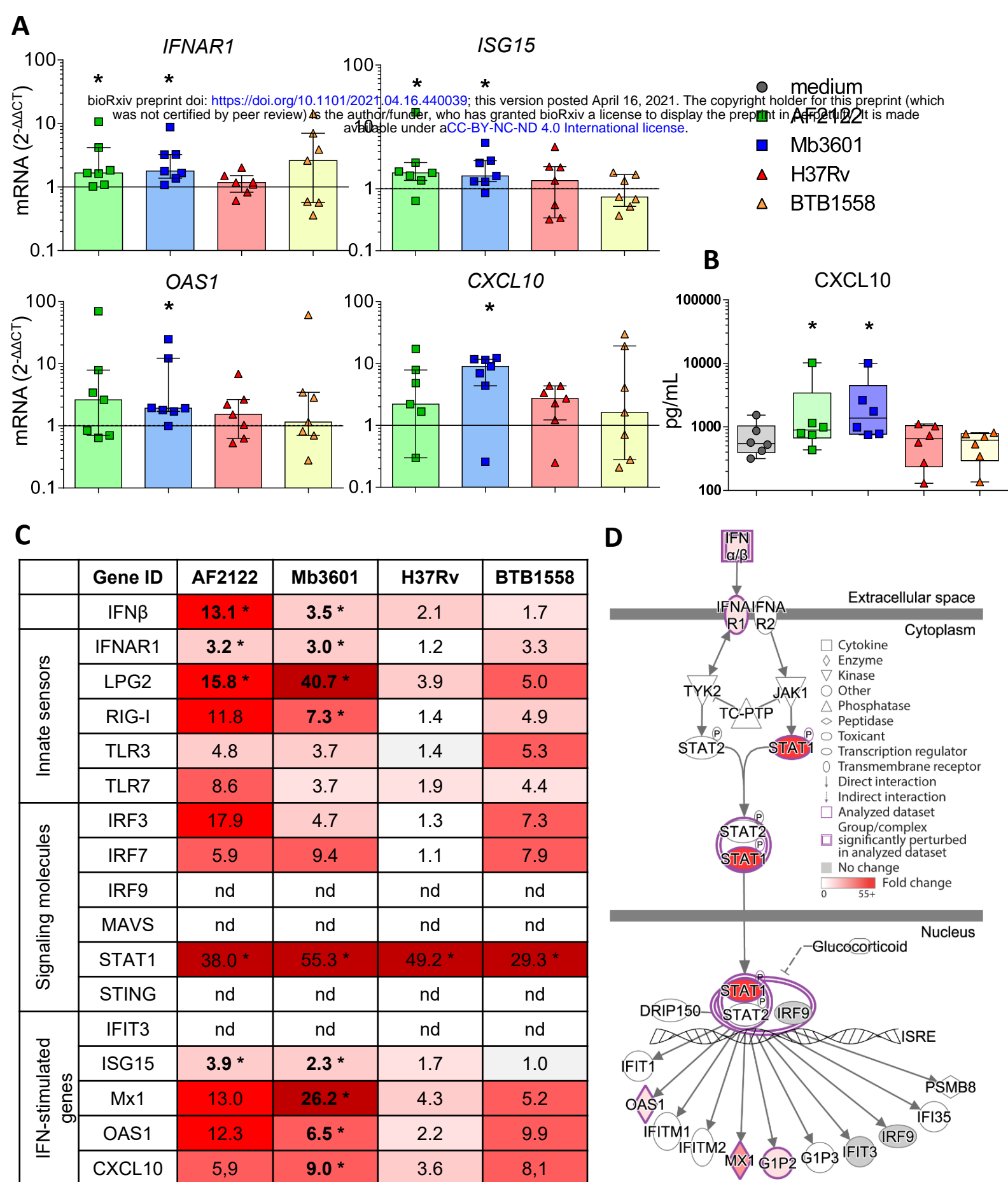
Figure 5: Mb but not Mtb infection in the lung tissue from Blonde d'Aquitaine cows induces the type I interferon pathway.

PCLS were infected as described in Figure 1. **(A)** *IFNAR*, ISG15*, CXCL10* and *OAS1* gene expression at 2 dpi. Individual data and the median and interquartile range in each group are presented (n=7) **(B)** CXCL10 protein level was measured in PCLS supernatant at 2 dpi. Individual data and the median and interquartile range in each group are presented (n=6). **(C)** The table represents the mean of fold change (2^{-ddCT}) for each group (n=7) of major genes involved in type I interferon pathway. Graduated red box coloring are for higher gene expression and asterisks mark significant differences compared to uninfected PCLS. nd=not detected. **(D)** Ingenuity Pathway Analysis drawing of the Type I interferon pathway under IFNAR in the Mb3601 group. Graduated red box coloring are for higher gene expression. (A, B and C) * $p<0.05$ (Wilcoxon non parametric test).
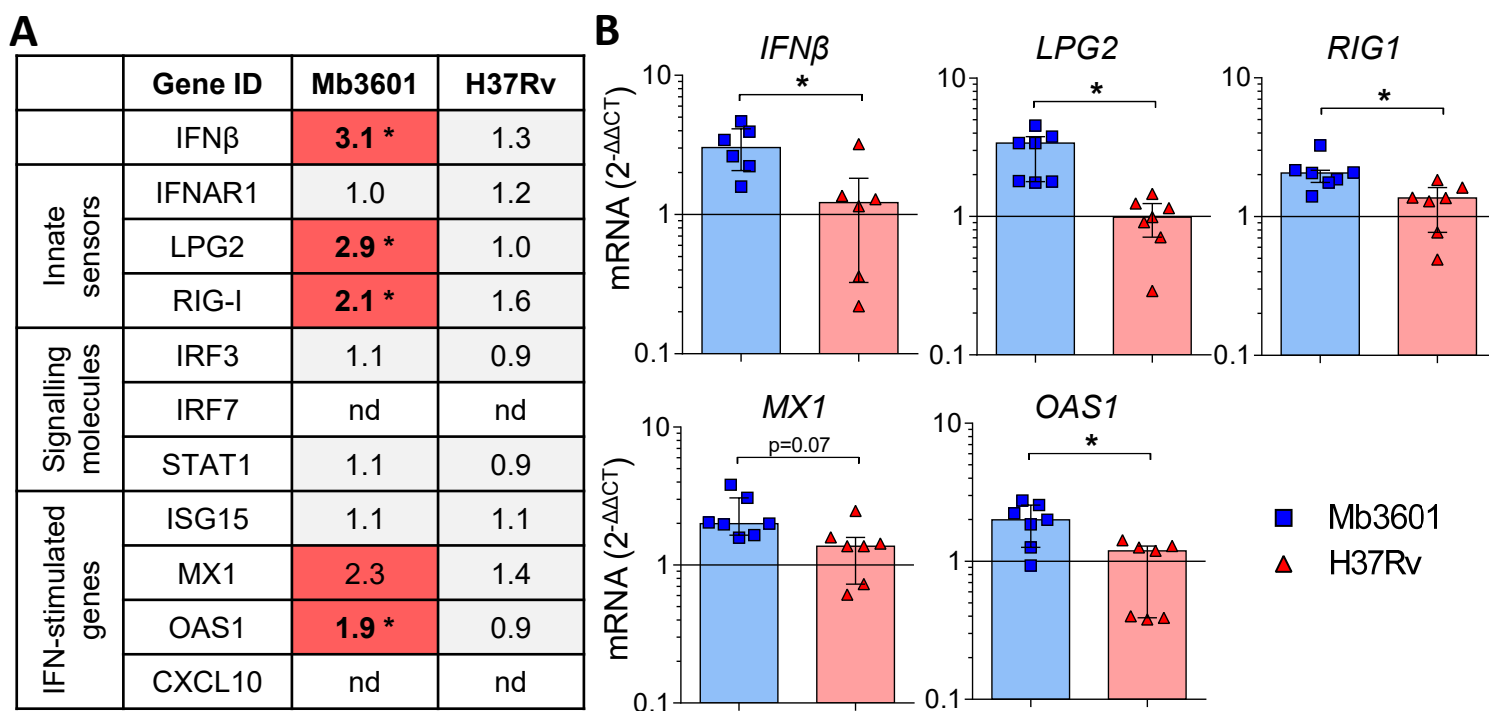
A

	Gene ID	Mb3601	H37Rv
	IFNβ	**3.1 ***	1.3
Innate sensors	IFNAR1	1.0	1.2
	LPG2	**2.9 ***	1.0
	RIG-I	**2.1 ***	1.6
Signalling molecules	IRF3	1.1	0.9
	IRF7	nd	nd
	STAT1	1.1	0.9
IFN-stimulated genes	ISG15	1.1	1.1
	MX1	2.3	1.4
	OAS1	**1.9 ***	0.9
	CXCL10	nd	nd

Figure 6: Alveolar macrophages from Blonde d'Aquitaine contribute to the type I IFN signature in lung induced by Mb infection

AMPs from Blonde d'Aquitaine lungs were infected with 10^5 cfu of Mb3601 or Mtb H37Rv. 6 h later mRNA was extracted from and expression of major genes from the type 1 IFN pathway was analyzed **(A)** Mean fold change (2^{-ddCT}) of gene expression normalized to three house keeping genes was calculated in each group (n=7). Graduated red box coloring represents gene expression and asterisks mark significant differences compared to non infected controls (nd=not detected). **(B)** *IFNβ*, *LPG2*, *RIG1*, *MX1* and *OAS1* gene expression in AMPs was analysed by RT-qPCR at 6h post infection. Individual data and the median and interquartile range in each group are presented (n=7). **(A, B)** * $p<0.05$ (Wilcoxon non parametric test).

★ Mb outbreaks (12.2019 - 12.2020)
■■ Blonde d'Aquitaine (>10000; 5-10000 cows)
■■ Charolaise (>20000; 10-20000 cows)
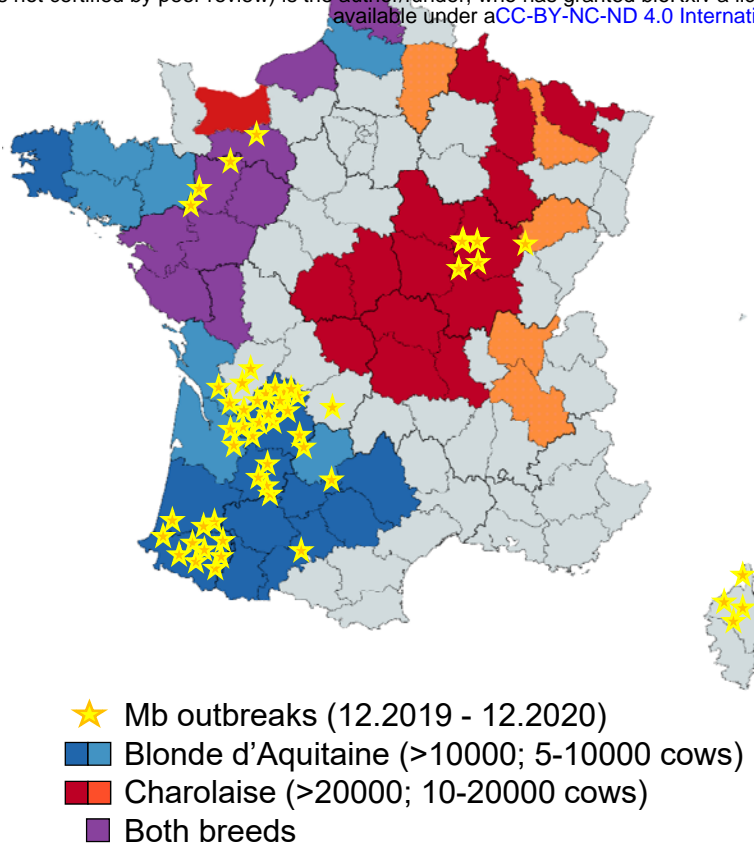■ Both breeds

Figure 7: Superposition of Blonde d'Aquitaine and Charolaise beef breeds in French counties where Mb outbreaks were declared between December 2019 and 2020.
This map of France shows counties where Mb outbreaks were declared between December 2019 and December 2020 (yellow stars) and was obtained with data extracted from https://www.plateforme-esa.fr/. Herd densities of Blonde d'Aquitaine (blue), Charolaise (red) or both breeds (violet) were extracted from data obtained from https://www.racesdefrance.fr (cows above 3-years-old have been considered).